

# UC San Diego

## UC San Diego Electronic Theses and Dissertations

### Title

A model within a model: Employing a simple community to unearth molecular mechanisms that mediate tripartite interactions between bacteria, phage, and fungi

### Permalink

<https://escholarship.org/uc/item/5zp1k5sk>

### Author

Spencer, Tara

### Publication Date

2023

Peer reviewed|Thesis/dissertation

UNIVERSITY OF CALIFORNIA SAN DIEGO

A model within a model: Employing a simple community to unearth molecular mechanisms that mediate tripartite interactions between bacteria, phage, and fungi

A Dissertation submitted in partial satisfaction of the requirements  
for the degree Doctor of Philosophy

in

Biology

by

Tara C.J. Spencer

Committee in charge:

Professor Rachel J. Dutton, Chair  
Professor Justin Meyer  
Professor Sonya Neal  
Professor Gentry Patrick  
Professor Joseph Pogliano  
Professor David Pride

2023

Copyright

Tara C.J. Spencer, 2023.

All rights reserved.

The Dissertation of Tara C.J. Spencer is approved, and it is acceptable in quality and form for publication on microfilm and electronically.

University of California San Diego

2023

## **DEDICATION**

This dissertation is dedicated to my parents Cleofoster and Josie Ann Spencer, my devoted sisters Ilya and Joni, and to the memories of my late, loving grandmother, Ms. Veronica Henry, and my bubbly, irreplaceable mentor Dr. Gary Heussler. Finally, I dedicate this dissertation to Jonathan Drakes, my husband-to-be, and the light of my life. The work described here is, in short, a fulfillment of the dreams they hold for me.

## TABLE OF CONTENTS

DISSERTATION APPROVAL PAGE	iii
DEDICATION	iv
TABLE OF CONTENTS	v
LIST OF FIGURES	vi
LIST OF TABLES	viii
ACKNOWLEDGEMENTS	ix
VITA	x
ABSTRACT OF THE DISSERTATION	xi
CHAPTER 1	1
CHAPTER 2	13
CHAPTER 3	27
CHAPTER 4	57
REFERENCES	61

## LIST OF FIGURES

Figure 2.1. **Hafnia-phage interactions take place within cheese rinds.** Included in the investigation of *Hafnia*-phage interactions were (A) bloomy rind and (B) washed rind *Hafnia* and phage isolates. (C) Actual plaque formation of cheese phages on lawns of 4 *Hafnia* strains. 5  $\mu$ L of serially diluted suspensions of pure phage were spotted onto each bacterial lawn. (D) Summary of phage plaquing data on *Hafnia* strains. Phages from one washed rind cheese (W1) and one bloomy rind (B1) cheese interact with *Hafnia* in modules: the phages that kill H1 hosts never kill H2 hosts, and vice versa. Page 23

Figure 2.2. **Genetic comparison of *Hafnia* phage genomes.** (a) *Hafnia* phages within each group have a higher pairwise AAI (over 99%) to one another than they do to phages outside that group. (b) *Hafnia* phages cluster into H1 and H2 infectivity groups based on their genomic similarity. Page 24

Figure 2.3. **Genetic comparison of *Hafnia* strains.** (A) Cheese *Hafnia* strains within each group meet a higher pairwise ANI (over 95%) to one another than they do to strains outside the group. (B) Cheese *Hafnia* strains cluster into H1 and H2 susceptibility groups based on the alignment of their RNA polymerase beta (*rpoB*) genes. Non-cheese *Hafnia* strains are included for comparison. Page 25

Figure 2.4. **CRISPR systems within *Hafnia* strains used in cheesemaking.** (A) Both H1 and H2 hosts have CRISPR arrays but only H2 hosts encode Cas enzymes. H1 spacers target the Curli prophage region within H1 genomes. Three H2 spacers target the Curli prophage region in the H1 genome. (B) Mauve alignment of Curli prophage and TS33 or TS42 genomes. Red or green vertical lines within boxes indicate regions of genomic similarity. Curli prophage is genetically distinct from TS33 and TS42 genomes. Page 26

Figure 3.1. **Novel lytic JB232-infecting bacteriophage TS33 is phylogenetically related to members of virus family Siphoviridae.** (A) Actual plaquing of JB232 phage on *Hafnia* lawn. 3  $\mu$ L of serially diluted suspensions of pure phage lysates were spotted onto a JB232 lawn. (B) Proteomic tree showing the predicted phylogenetic classification of TS33 among Siphoviridae. Phylogeny was determined based on whole genome comparison of the TS33 proteome to the proteomes of well-characterized bacteriophages using the Viral Proteomic Tree (ViPTree) Server. Page 47

Figure 3.2. ***Hafnia* library growth is inhibited in the presence of a community of fungi and bacteriophages.** The *Hafnia* sp. JB232 library was grown alone, and with phage and/or fungi on *in vitro* cheese medium for three days. The harvested cells (A), spores (B,C) and phage particles (D) were plated on each day and quantified using the total number of cfus and pfus respectively. Page 48

Figure 3.3. **Mutations in genes controlling O-antigen synthesis and ligation may exhibit pleiotropic effects.** (A) The barcodes of the *Hafnia* library plated under various growth conditions were amplified and sequenced. The original RB-TnSeq bioinformatic pipeline developed by Wetmore et al. (2015) was used to quantify each barcode and determine the

abundance of each mutant in each gene represented in the library. The sum of the abundances of each mutant for each gene was used to assign a fitness value to each gene. Mutations with a significant negative and positive fitness effect are represented in burgundy and blue respectively. (B) The number of genes unique to and shared by the 4 growth conditions were determined using the UpSet R function developed by Conway et al. (2017). (C) The KEGG Mapper was used to identify gene pathways enriched under each condition. (D) ComplexHeatMap in R was used to compare the enriched genes under each condition. (E) Schematic representation of *rfa* operon in *Hafnia* JB232 Wildtype. Adapted from Pagnout et al. (2019). Page 49

**Figure 3.4. LPS mutations increase *Hafnia* sp. JB232 resistance to TS33 infection but decrease bacterial growth in the presence of the fungi.** (A) Comparing phage infectivity of WT and mutant strains. Phage infectivity is measured by the number of TS33 phage particles (shown here as the number of plaque forming units/pfus) produced following infection on a soft agar lawn of each bacterial strain. (B) Effects of fungi on growth of *Hafnia* strains over 3 days, measured in the number of viable bacterial cells (represented here in colony forming units (cfus)). (C) Images of phage plaquing on various *Hafnia* mutants. Page 50

**Supplementary Figure 3.1. Genomic analysis and manipulation of cheese bacterial strain JB232.** (A) Genome Based Distance Phylogeny (GBDP) tree based on genome data reveals that JB232 forms a unique species cluster within the genus *Hafnia*. Phylogeny was determined using the Type (Strain) Genome Server (TYGS) and the tree was visualized using Interactive Tree of Life (iTOL). (B) Insertion map of JB232 genome library. The RB-TnSeq library was constructed in the laboratory via conjugation with *Escherichia coli* strain APA766 carrying the pKMW7 Tn5 vector library (Wetmore et al. 2015). Each vertical bar in the map represents the number of insertions within a 1000 bp region; bar height is directly proportional to the number of insertions, with approximately 1700 insertions being represented by the longest bar. Library sequencing revealed 103169 insertions in 58869 distinct locations within the JB232 genome. These insertions occur within the central 10-90% of each represented gene. The RB-TnSeq library contains mutants in approximately 88% of the protein-coding genes, each of which has an average of 25.6 strains. The insertion map was visualized using Anvi'o. Page 51

**Supplementary Figure 3.2. Comparison of significant gene fitness values for the individual replicates in each experimental condition.** (A) Principal Component Analysis was conducted on the significant gene fitness values using the `prcomp()` function in Rstudio. (B) We identified genes of significant fitness unique to and/or shared by the three replicates from four growth conditions using the UpSetR package in Rstudio (Lex et al. 2014, Conway et al. 2017). Page 52

**Supplementary Figure 3.3. Determining the normality of the data sets visualized in Figure 3.4.** (A) Under all tested conditions, the number of *Hafnia* colony forming units follows a normal distribution based on Shapiro-Wilk (S-W) and Pearson Chi-Squared Normality tests ( $p > 0.05$ ). (B) The number of plaque-forming units of TS33 does not follow a normal distribution based on the shape of the quantile-quantile plot ( $p < 0.05$ ). Page 53

## LIST OF TABLES

Supplementary Table 3.1. ***Hafnia* sp. JB232 mutants isolated from barcoded transposon mutant library.** All mutants have mutations in genes related to LPS biosynthesis. *Page 54*

## ACKNOWLEDGEMENTS

I take this opportunity to acknowledge my strong support system who has carried me during this process. I send a special thank you to my fiancé Jonathan Drakes for his unending affirmations and prayers that elevated me amid long nights and failed experiments. I thank my family: my parents and sisters, Ilya and Joni, whose love and jovial conversations kept me going through this time. I thank my chosen family of Precision Centre and Sent Life Centre for always carrying me in their hearts and uplifting me with their bounteous words.

I am especially grateful for the Dutton lab: Steven, Brooke, Manon, Emily, Christina and my bright-eyed mentee, Angel. Thank you all for useful conversations, troubleshooting and encouraging me when there were roadblocks. Thank you, Angel, for embarking on this fruitful yet bumpy journey with an inept navigator. Thank you for trusting me, and for contributing significantly to my doctoral dissertation.

I reserve this spot for a special thanks to my amazing mentor, Dr. Rachel Dutton. When I first joined the Dutton Lab, I was a young and spritely scientist with new ideas and an unknown path forward. Rachel supported every single step of my journey which has led me to this day. I could and can still always count on Rachel's resounding "yes" to each endeavor that I have embarked on. It was her holistic support of my entire wellbeing that created the ideal environment for me to advance scientifically and arrive at the findings that are shared in this document.

Thank you, Rachel, for taking a chance on an inexperienced black girl from the Caribbean and giving her a fast track to success in science.

"Chapter 3, in full, is currently being prepared for publication. The dissertation author was the primary research/author of this paper."

## VITA

2018 Bachelor of Science in Biology, Howard University

2023 Doctor of Philosophy in Biology, University of California San Diego

## **ABSTRACT OF THE DISSERTATION**

A model within a model: Employing a simple community to unearth molecular mechanisms that mediate tripartite interactions between bacteria, phage and fungi

by

Tara C.J. Spencer

Doctor of Philosophy in Biology

University of California San Diego, 2023

Professor Rachel J. Dutton, Chair

Diverse and widespread populations of bacteriophages infect and co-evolve with their bacterial hosts. Although the process of host recognition and infection occurs within microbiomes, the molecular mechanisms underlying host-phage interactions within the context of a community remain poorly studied. The biofilms, or rinds, of cheese, contain taxonomically diverse microbial

communities that follow reproducible growth patterns and can be manipulated under laboratory conditions. Our lab has previously used a model Brie community to demonstrate specific microbe-microbe interactions occurring within a community. Using this system, we are investigating how host-phage interactions and co-evolution influence other community members, and vice versa. The work outlined here described our efforts to use cheese as a model for studying phage-microbe interactions by identifying and characterizing a tractable host-phage pair co-occurring within this system. We successfully isolated lytic bacteriophage TS33 that kills *Hafnia* sp. JB232, a member of a model Brie community. TS33 is easily propagated in the lab and naturally co-occurs in the cheese with its *Hafnia* host and other members of the Brie community, rendering it a prime candidate for the study of host-phage interactions. We used Random Barcode Transposon Sequencing (RB-TnSeq) experiments to identify candidate host factors that contribute to TS33 infectivity, many of which are critical to the integrity of the lipopolysaccharide (LPS) layer of the host cell. Notably, disruption of these genes results in decreased susceptibility to infection by phage TS33, while simultaneously exhibiting a significant negative effect on the fitness of *Hafnia* sp. JB232 in the presence of its fungal partners, *Geotrichum candidum* and *Penicillium camemberti*. Therefore, LPS mutations may have pleiotropic effects on the interactions between *Hafnia* sp. JB232 and the rest of the Brie community. Ongoing and future studies aim to unearth the molecular mechanisms by which the LPS of *Hafnia* sp. JB232 mediates its interactions with its viral and fungal partners.

## CHAPTER 1

**Authors: Tara C.J. Spencer<sup>1</sup>, Rachel J. Dutton<sup>1</sup>**

<sup>1</sup>Division of Biological Sciences, Section of Molecular Biology, University of California San Diego, 9500 Gilman Drive, La Jolla, CA, 92093, USA

### **1.1 Bacteria-phage interactions within simple microbial communities**

The most abundant replicating entities within our biosphere are bacteriophages or phages, viruses that infect and kill bacterial cells. There are an estimated  $10^{31}$  phage particles on Earth (Comeau et al., 2008). Despite their small size, they possess unique life cycles which provide myriad opportunities to interact with and profoundly impact their hosts. Bacteriophages and their hosts boast an extraordinary genetic diversity, suggesting that host-phage interactions are multifarious (Kauffman et al., 2022, Jessup & Forde 2008). The detailed mechanisms of several host-phage interactions have been extensively documented, revealing their robust impacts on host biology.

**Phage effects on bacterial abundance.** Microbial diversity is a measurable outcome of host-phage interactions (López-Leal et al., 2022). Lytic bacteriophages control host abundance in a density-dependent manner. For instance, a 2015 metagenomic study revealed that bacterial abundance, and thus disease pathogenesis, in patients of Crohn's disease, ulcerative colitis, and inflammatory bowel disease is maintained in a phage density-specific manner (Norman et al., 2015). Interestingly, despite the dependence of phage titers on host abundance, high bacterial load was not proportional to viral titer.

Lysogenic phages may also positively influence the fitness and therefore density of their hosts within a community through various mechanisms. For instance, protection from

superinfection is a common benefit of lysogeny to the host (Bondy-Denomy et al., 2016). In various Gram-Negative bacteria, the prophage-encoded anti-phage protein BstA curtails the infection cycle of lytic phages (Owen et al., 2021). A similar example is seen in *Vibrio cholerae* where the nuclease activity of the prophage-encoded phage parasite, Nix1, prevents phage genome replication and packaging in vitro (LeGault et al., 2022). Additionally, the virulence factors of various pathogens like Shiga toxin-producing *E. coli* (STEC), *Clostridium botulinum*, and *Vibrio cholerae* are all encoded by lysogens in the bacterial genome (Habets et al., 2022, Fortier 2017, Huang et al., 1987). Lastly, bacterial hosts commonly benefit from the transduction of advantageous genes. In poultry-associated commensal *Salmonella* spp., for instance, genes required for bacterial adherence to host cells are prophage-encoded (Yu et al., 2022).

**Phage effects on host gene expression.** After decades of coevolution with their hosts, bacteriophages have devised methods of controlling bacterial gene expression. The very foundation of lytic infection is a redirecting of the host biosynthetic machinery to their genetic material (Warwick-Dugdale et al., 2019, Chaikeratisak et al., 2017). For many bacteria, this reprogramming comes at a cost to the host. Under most conditions, lytic phage infection results in bacterial cell lysis (Zdrojewska et al., 2019). In unique cases, host energetics can be reprogrammed to suit the bacteriophage. Cyanophages, like P-HM2, have a remarkable interaction with their hosts. While dependent on their host *Prochlorococcus* for nucleotide biosynthesis, phages S-PM2 and P-HM2 encode genes required for bacterial light-harvesting and photosynthetic electron transport (Sharon et al., 2009; Alperovitch-Lavy et al., 2011, Mann et al. 2003). Interestingly, P-HM2 mediates electron flux in its host during photosynthesis by controlling the expression of photosynthetic electron transport genes in their hosts to favor

themselves (Thompson et al., 2015). Other marine phages have been found to upregulate nucleotide biosynthesis gene expression in their hosts following infection (Enav et al., 2014).

Quorum sensing is a cell-cell communication system used by bacteria to coordinate internal gene expression levels. In *Pseudomonas aeruginosa*, quorum sensing is used to facilitate population-wide CRISPR-Cas activation and elimination of phage under high cell densities (Høyland-Kroghsbo et al., 2017). However, *P. aeruginosa* phage DMS3 expertly manipulates biochemical pathways involving quorum sensing to produce two negative consequences for the host (Shah et al., 2021, van Kessel and Mukherjee 2021). The phage protein Aqs1 inhibits the regulation of quorum sensing by blocking LasR activity in *P. aeruginosa*. Subsequently, any anti-phage defense systems mediated by quorum sensing are effectively blocked. As an example, Aqs1 can promote superinfection by blocking the anti-phage activity of type IV pilus in the host. In this way, DMS3-*P. aeruginosa* interactions result in more successful host infections by the phage.

Bacteriophages can also influence host lifestyles and the availability of resources in the environment. For example, most bacteria in nature grow in biofilms, a state which offers a high level of protection from harsh external stimuli. Under low phage densities, the expression of genes required for biofilm formation is promoted in *Staphylococcus aureus* (Fernandez et al., 2017). Similarly, *Prochlorococcus*-phage interactions may benefit other species in the same environment. Cyanophage infection can stimulate the host to release outer membrane vesicles, an event that is critical to carbon flux in marine contexts (Biller et al., 2014, Mozaheb & Mingeot-Leclercq 2020, Silva et al., 2022).

**Phage effects on bacterial diversity and evolution.** There are numerous examples of the role of host-phage interactions on bacterial diversification (Williams et al., 2013). In some systems, fluctuating selection can be observed where abundant bacterial strains coevolve with their phages. This kill-the-winner model can proceed as follows: phages can more easily target faster-growing cells, thus lowering their abundance; subsequently, resistant cells emerge with high fitness and bacterial abundance increases (Kortright et al., 2022, Rodriguez-Valera et al., 2009, Meyer et al., 2012). In this way, antagonistic interactions between bacteria and phages can select for highly diverse populations of bacteria with varying levels of susceptibility to the phages present (Scanlan et al., 2017). As a matter of fact, the more antagonistic the interactions, the more diverse the population is predicted to be (Maslov and Sneppen, 2017).

Host evolvability is a well-studied consequence of phage infection. Diverse bacterial populations may experience accelerated mutation rates in the face of perturbations by phage (Paterson et al., 2010, Cairns et al., 2017). In a 2015 study, Scanlan et al. observe increases in mutations throughout the entire genome of *Pseudomonas fluorescens* following 400 generations of coevolution with bacteriophage Phi2 (Scanlan et al., 2015). Therefore, by driving variability within a population, phage-driven bacterial diversification directly impacts host evolvability.

To evade their viral predators, bacterial hosts have evolved an astonishing number of evolutionary pathways (Koskella and Brockhurst 2014). A ubiquitous phage-defense mechanism and common target in the bacteria-phage evolutionary arms race is CRISPR-Cas adaptive immunity (Watson et al., 2021). CRISPR systems enable bacteria to detect and degrade injected phage genomes, aborting successful phage infection (Mojica et al., 2015). Initially, genetic material from successful phage infection can be incorporated into the CRISPR loci of the infected cell (Amitai et al., 2016). These “spacers” can then be used to guide the Cas-mediated

degradation of any foreign genetic elements, like phage DNA, containing the target sequence (Garneau et al., 2010). During coevolution, CRISPR systems can rapidly evolve to favor the bacterium in the host-phage arms race (Broniewski et al., 2020). Additionally, a combination of metagenomics and *in vitro* experimentation has been recently used to identify 21 novel anti-phage mechanisms which are ubiquitously encoded in bacterial genomes. Some of these molecular pathways involve genes that are homologous to human innate immunity genes (Millman et al. 2022). They found that induced expression of the ubiquitin-like protein, ISG15, defended bacteria from 5 genera against infection from several different phages. Additionally, genes involved in polynucleotide manipulation, membrane remodeling, and toxin-antitoxin systems were linked to phage defense. Guo et al. also unearthed the role of membrane remodeling in phage resistance in *Bacillus subtilis*, via a bacterial dynamin-like protein (Guo et al. 2022).

Moreover, bacteria commonly employ absorption-blocking phage-resistance mechanisms (Rostøl and Marraffini 2019). Many phages exploit bacterial cell-surface proteins during their life cycle. As a first line of defense, phage receptors are often mutated, quickly leading to phage extinction (Labrie et al., 2010). Meyer et al. provide a clear example where predation by lambda phage selects for *E. coli* mutants in the LamB receptor, resulting in decreased fitness in the phage population (Meyer et al., 2012). Additionally, several phages adsorb to the lipopolysaccharide (LPS), a cell-surface glycolipid that protects Gram-Negative bacteria from chemical, bacterial, and viral attacks (Bertani and Ruiz 2018). Thus, the LPS is another target for phage resistance; *E. coli* has been a useful model for demonstrating the benefit of inhibiting LPS synthesis in light of phage attack (Burmeister et al., 2020, Zhong et al., 2020, Kulikov et al., 2019, Hancock and Peeves 1976).

The diverse interactions between bacteriophages and their hosts occur within consortia called microbiomes, microscopic hubs for microbial interactions and competition. Microbiomes occupy virtually every niche on Earth, from the soil to the human gut, and microbes often form essential symbioses with multicellular life. Extensive studies have shown the large impacts of diverse microbial communities in biogeochemical cycling, vector-dependent disease transmission, immunity, neurological function, and even adaptation to harsh environments (Falkowski et al., 2008, Fung et al., 2017, Urakova et al., 2022, Walker et al., 2011). Microbial communities are crucial to modern life on Earth, as seventy percent of atmospheric oxygen is generated by marine microbial species (Sekerci et al., 2015).

As the sites of phage replication and evolution, the community context of host-phage interactions is indispensable to a complete understanding of phage biology. We are still limited in our understanding of how ecological partners affect host-phage interactions; however, recent publications have begun to address this question.

**Community impacts on host and phage abundance.** Current data from various groups suggest that the presence of a community may limit host-phage interactions. In two separate experiments involving communities from soil and human lung ecosystems, scientists observed that growth in a community context led to the suppression of bacterial and phage densities. In a study by Gomez and Buckling, *P. fluorescens* SBW25 was cultured with its natural soil community and/or bacteriophage SBW25 $\phi$ 2 in sterilized soil (Gómez & Buckling 2011). In the presence of the community, both bacterial and viral growth was inhibited. Moreover, a polymicrobial lung infection model has been used to show the negative impacts of community presence on bacterial and phage growth (Mumford & Friman 2016). Any or all community

members were sufficient to depress the growth of *P. aeruginosa* and lytic phage PT7 isolated from wastewater was and their respective phages. Interestingly, in both cases, the absence of the community led to a significant increase in the mean density of the pseudomonads under study. Additional work further exposes the negative effects of a model infection community on the growth of phage DMS3vir (Alseth et al., 2019). In stark contrast to these findings, Johnke et al. reveal a protective effect of a generalist protist community on host density. In their experiments, *Klebsiella* sp. successfully coexisted with the bacteriophage in the presence of the community (Johnke et al., 2017). To our knowledge, the molecular mechanisms whereby any of the observed effects of the community on host/phage growth have not yet been discovered (Blazanin and Turner, 2021).

**Community impacts on host-phage interactions.** Johnke et al. found that the suppressive effects of the community on *Klebsiella* sp. are exacerbated when phage is present (Johnke et al., 2017). Due to the lytic nature of the phage, *Klebsiella* sp. abundance is lower when the phage is around. However, in the presence of specific community members, host abundance is maintained. This is not always the case, as the community offers a positive effect on *P. fluorescens* growth under conditions of phage predation (Gómez & Buckling 2011). A similar effect is also observed in the PT7-*P. aeruginosa* interactions within an infection community; however, competition and host genotype appeared to play an additional role in the effects of PT7 predation on *P. aeruginosa* (Mumford & Friman 2016). Due to the conflicting nature of these results, more experimentation involving host-phage interactions from various species is necessary to certify the effects of community presence therein.

**Community impacts on host-phage coevolution.** As mentioned above, bacteria often evolve evasive strategies in the presence of phage. Subsequently, counter-resistance mutations

emerging in the phage population enable them to reinfect their hosts. Therefore, hosts and phages exist in an evolutionary arms race, resulting in observed flux in their resistance and infectivity respectively (Meyer et al., 2012).

There is evidence that community presence can constrain, support, or have no effect on the coevolutionary dynamics of bacteria and their phages (Blazanin and Turner, 2021). Johnke et al. and Mumford and Friman independently find that community presence limits the frequency of host adaptation to phage predation (Johnke et al., 2017, Mumford & Friman 2016). Yet, quorum-sensing deficient *P. aeruginosa* was still able to adapt to PT7 predation, suggesting the host genotype-specificity of community effects on host-phage coevolution. Some microbial communities do not significantly impact host adaptation to phage. Middelboe et al. explore the effects of marine communities on four bacteria-phage pairs, in which they find that viral lysis of the host was combated by phage resistance in every community context (Middleboe et al., 2001). In another study, De Sorti et al. conduct an investigation of the coevolutionary dynamics between *E. coli* phage P10, a susceptible host, and a resistant host within the mouse gut. They show that P10 can only evolve to infect the resistant host in the presence of the conventional mouse microbiome by interacting with a strain of *E. coli* that is native to mice (De Sorti et al., 2019, De Sorti et al., 2017). Their findings suggest that community context significantly impacts the evolutionary trajectories of phage interacting with bacteria. Evidently, we are still limited in our understanding of how ecological partners affect host-phage interactions, especially their coevolution.

In addition to having a limited understanding of community impacts on host-phage interactions, we have almost no information about the molecular mechanisms that underlie these interactions. Perhaps the only mechanistic insight is offered by Johnke et al., who present a

potential role of quorum sensing and competition in mediating host adaptation to phage predation (Johnke et al., 2017). However, there is evidence that environmental pressures (which can originate from microbial partners) have adverse effects on the adapted host.

As previously mentioned, bacterial adaptations to phage predation typically rely on targeting host immunity and phage adsorption sites (LPS or cell-surface receptors). In some cases, these adaptations are likely to come at a cost to the bacterium, including deleterious impacts on competitiveness and carbon metabolism, as well increased susceptibility to other phages and antibiotics (Middelboe et al., 2009, Avrani et al., 2011; Marston et al., 2012, Brookhurst et al., 2005).

In another study of *E. coli*-phage interactions, Burmeister et al. observe that resistance to phage U136B is conferred by mutations in the two structures that confer antibiotic resistance: the LPS and the efflux pump, *tolC* (Burmeister et al., 2020). By targeting these adsorption sites, the bacterium is now rendered susceptible to antibiotic attack. These LPS disruptions are believed to destabilize the cell wall structure, resulting in increased permeability to various antimicrobials, and potentially, other bacteriophages (Pagnout et al. 2019). Similar LPS mutations increase sensitivity to sodium dodecyl sulfate (Zhong et al., 2020). The antagonistic pleiotropy associated with phage resistance mechanisms is also observed in *Pseudomonas aeruginosa*, where phage-selected mutations in the OprM protein increase host susceptibility to multiple antibiotics (Chan et al., 2016). Therefore, in an environment containing antimicrobials, resistance adaptations can be expected to have deleterious consequences for the host.

At the same time, there is evidence that synergistic pleiotropy in LPS genes is possible, even in a tumultuous environment. In a 2023 study, the antibiotic susceptibility of four *E. coli* mutants in different cassettes involved in LPS synthesis was tested (McGee et al., 2023). Only 1

of these mutants exhibited increased susceptibility to antibiotics, while the remaining 3 were resistant to antibiotics. As a matter of fact, two of them were significantly more resistant than the wildtype. Altogether, these findings suggest that the fitness benefit of phage resistance mechanisms may be context-dependent and gene-specific.

As we continue to grow our understanding of the impact of community context on host-phage ecology and coevolution, it is essential that we pursue the molecular basis of observed host-virus-community interactions, and that we conduct these experiments using a realistic ecological timeline. Many of the studies discussed before employ a short-term time scale of up to 15 generations. It is likely that the absence of a tractable system within which to conduct these experiments has impeded our ability to approach questions about host-phage-community ecology and evolution. Most microbiomes have a high species diversity, making it impractical or even impossible to perform experiments involving the entire community. Additionally, our inability to culture the majority of the microorganisms associated with a community in the lab further complicates efforts to study microbial interactions using culture-dependent approaches.

The Dutton lab has developed cheese as a model system for microbiome studies (Wolfe et al., 2014). The biofilms, or rinds, at the surface of aged cheese, contain simple yet taxonomically diverse microbial communities that follow reproducible growth patterns and can be manipulated under laboratory conditions. Consequently, we have achieved successful *in vitro* community reconstruction of the microbiomes associated with washed and bloomy rind cheeses (Saak et al., 2023, Morin et al., 2018).

Employing culture-dependent and culture-independent approaches to cheese communities has revealed key biological and molecular processes that take place within microbiomes (Saak et

al., 2023, Morin et al., 2022, Morin et al., 2018, Bonham et al., 2017, Pierce et al., 2020). One such process is horizontal gene transfer (HGT), a major driver of evolution and niche adaptation (Wiedenbeck and Cohan, 2011). Using a custom-made computational pipeline, extensive horizontal gene transfer (HGT) was revealed within cheese microbial communities, particularly of genes related to nutrient acquisition and metabolism, information processing, and energy metabolism (Bonham et al., 2017). Additionally, cheese contains a diversity of mobile genetic elements via which HGT is likely to occur, such as diverse bacteriophages and plasmids (Saak et al., 2023).

Simple cheese communities have also proven useful for investigating the effect of community complexity on bacterial genetic requirements. The community of *Hafnia* sp. JB232, *Geotrichum candidum*, and *Penicillium camemberti*, three typical partners in a bloomy rind cheese (Morin et al., 2018), has been particularly useful in dissecting mechanisms within a community. Using transposon insertion mutant libraries of *E. coli* and *Pseudomonas psychrophila*, the metabolic interactions driving the growth of each bacterium within the community were probed. For both species, competition for iron and nitrogen, as well as cross-feeding of amino acids from fungal partners, were dominant interactions observed. Interestingly, these fungal partners and 6 others were found to regulate iron and biotin availability for both bacterial species (Pierce et al., 2020). Moreover, the impact of *E. coli* and *P. psychrophila* are significantly impacted by both pairwise and higher-order interactions. As a matter of fact, increasing community complexity leads to the disappearance of most of the pairwise interactions, leading to the emergence of higher-order interactions (Morin et al., 2022, Morin et al., 2018). In other words, community complexity reshapes the genetic requirements and microbial interactions taking place within even a simple microbiome.

All in all, the cheese microbiome is a useful model from which we can glean insight into the molecular mechanisms that underlie interactions within a community. However, the experimental tractability of this system has yet to be leveraged for studying the contributions of a simple community to virus-host interactions, and vice versa. As discussed previously, the literature has established the impact of several bacteriophages on host metabolism, diversification, and evolution. Introducing bacteriophages to our *in vitro* model provides a unique opportunity to investigate how the presence of a community affects these consequences of host-phage interactions. What is more, we can gain a full-scale view of the molecular processes taking place in the communities among cellular and acellular microbes.

This dissertation outlines the development of a “model within a model” for investigating the impact of community context on bacteria-phage interactions. We discover and introduce a novel bacteriophage that infects *Hafnia* sp. JB232 into our simple Brie microbial community. Leveraging our expertise in high-throughput genetic screens, we investigate the molecular impact of community context on host-phage interactions. The experiments outlined here (1) probe the role of ecological context on host-phage interactions, and (2) shed light on the molecular mechanisms that underlie the tripartite interactions between viruses, bacteria, and fungi within a simple community.

## CHAPTER 2

### Identifying model host-phage interactions within a model community

**Authors: Tara C.J. Spencer<sup>1</sup>, Angel Sarabia<sup>1</sup>, Gary Heussler\*, Steven Villareal<sup>1</sup>, Rachel J. Dutton<sup>1</sup>**

<sup>1</sup>Division of Biological Sciences, Section of Molecular Biology, University of California San Diego, 9500 Gilman Drive, La Jolla, CA, 92093, USA

\*deceased

### 2.1 Chapter Summary

Microbiomes are the primary sites of interactions and coevolution between bacteriophages and their bacterial hosts. Yet, the molecular mechanisms underlying these dynamics within the context of a community are poorly understood. Cheese biofilms, or rinds, are taxonomically diverse microbial communities that follow reproducible growth patterns. Moreover, cheese-associated microbes are easily manipulable in the laboratory. We have previously used a simple Brie community containing the bacterium *Hafnia* sp. JB232, the yeast *Geotrichum candidum*, and the mold *Penicillium camemberti*, to investigate how bacterial-bacterial and bacterial-fungal interactions occur within a community. In this study, we expand this model community to include *Hafnia* sp. JB232-infecting phage TS33 to investigate how host-phage interactions influence other community members and vice versa. To this end, we isolated 21 bacteriophages that reside in cheese and infect 4 *Hafnia* strains isolated from cheese or commonly used in cheesemaking. Comparative genomics reveals that the 4 strains belong to two different species of *Hafnia*. Moreover, the phages exhibit narrow host ranges, as they can only infect one species of *Hafnia*. Additionally, the phages that infect *Hafnia* sp. JB232 are

highly genetically similar, leading us to select TS33 at random for introduction into the model community. Interestingly, no *Hafnia* CRISPR systems target any of the phages under scrutiny, suggesting that some other genetic factors underlie *Hafnia*-phage interactions.

## **2.2 Isolating and taming phage candidates for the model host-phage interaction**

### **Introduction**

Viruses are perhaps the most abundant replicating entities on the planet. They are found in virtually every environment where life thrives - from the soil to the human gut. Some viruses are harmless and even beneficial to humans, while others are agents of disease (Koonin et al., 2012). Bacteriophages are viruses that can infect and kill bacterial cells, and thus they can have widespread impacts on ecosystems (Manrique et al., 2017, Pratama et al., 2018, Febvre et al., 2019, Homma et al., 2007, Meyer et al. 2012). Extensive research has revealed both their extraordinary genetic diversity and the detailed molecular mechanisms of their interactions and co-evolution with their bacterial hosts. What is missing from this literature, however, is a demonstration of the impact of a microbial community on these interactions, as well as an understanding of the impact of phage infection on a microbial community. Because viruses replicate and evolve within microbial communities, we may have missed key molecular components of viral biology by eliminating the community from these studies. I believe that an understanding of how these phenomena take place in a community context has the potential to reveal new principles underlying virus-host-community interactions.

The absence of a tractable system within which to conduct these experiments has impeded our ability to answer these questions. Most microbiomes have a high species diversity, and most of these microorganisms are not culturable in the lab. Our lab has developed cheese as

a model system for microbiome studies (Wolfe et al., 2014). The biofilms, or rinds, at the surface of aged cheeses, contain simple yet taxonomically diverse microbial communities that follow reproducible growth patterns and can be manipulated under laboratory conditions. Using this system, we have begun to elucidate the biological processes and molecular mechanisms that take place within microbiomes (Morin et al., 2018, Bonham et al., 2017, Pierce et al., 2020). The experimental tractability of this system has yet to be leveraged for studying tripartite virus-host-community interactions.

Here, we investigate the use of bacteriophages residing in cheese rinds as models for investigating the interactions that viruses have with other microbes within their community. Our bacterial host was identified based on its presence in our model Brie community of *Hafnia* JB232, *Geotrichum candidum*, and *Penicillium camemberti*. Using this model, we have shown that competition and cross-feeding are critical interactions for focal bacteria *Escherichia coli* and *Pseudomonas psychrophila* within this community (Morin et al., 2018). Moreover, we have demonstrated that core microbial interactions are reshaped by increasing community complexity (Morin et al., 2022, Morin et al. 2018).

We successfully isolated 21 bacteriophages that infect various strains of *Hafnia* used in cheesemaking. Based on the host range of the phage isolates, we focus our efforts only on those to which *Hafnia* sp. JB232 is susceptible, and utilize comparative genomics to select one to be used in our model host-phage interactions. Using this model, we can begin to approach the following questions: *Does the presence of a community affect the infection of a host bacterium by phage? Does phage infection of a host, in return, alter community structure and function? What are the molecular mechanisms underpinning phage-host interactions and do they change*

*in the presence of a community? What genetic or environmental factors permit phage persistence in communities? Does the presence of a community alter the course of phage-host coevolution?*

## **Results**

**Taming bacteriophages from cheese rinds.** Initially, our Brie community excluded bacteriophages; thus, we began by isolating a bacteriophage that infects the bacterial member of the community: *Hafnia* JB232. To maximize the number of phages under investigation and identify potential broad host-range candidates, we enriched phages that infect 4 of the *Hafnia* strains isolated from cheeses made at Jasper Hill Farm, VT: *Hafnia* strains JB232, VRAC, JH36 and JH591.

Phage lysates were obtained from the same cheeses in which these strains are inoculated. Specifically, we used a bloomy rind cheese from which JB232 was isolated, and a bloomy rind cheese (Figure 1A, B; Wolfe et al., 2014). Three rounds of quadrant streaking were used to purify bacteriophages. For each strain, we performed spot titer assays of each phage to determine viral host range.

**Determining host range of phages.** These plaque assays revealed varying sensitivity to the phages among the 4 *Hafnia* strains, such that the hosts can be grouped based on their susceptibility. JB232 and VRAC (referred to as H1 hosts) are killed by the same set of phages (Figure 1C, D). Conversely, JH36 and JH591 (referred to as H2 hosts) are killed by the remaining phages. Notably, the H1-infecting phages never kill H2 hosts and vice versa.

**Comparing genomes of *Hafnia* JB232-infecting phages.** Given the infection profile of the *Hafnia* phage isolates, I hypothesized that the H1-infecting phages would be genetically distinct from the H2-infecting *Hafnia* phages. We sequenced the 21 phage genomes, including 15 H1-

infectors and 6 H2-infectors. Phage genome comparison revealed that H1-infecting phages are clonal, having an average amino acid identity (AAI) of >99% to any other H1 infectors, and are genetically divergent from H2-infectors (Figure 2A). Notably, all phages have high genetic similarity to other phages within their group; we observe minimal genetic divergence within each group. Indeed, these two groups of phages share no regions of genomic similarity. As a matter of fact, whole genome comparisons using ViPTree predict the H1-infecting phages to be *Siphoviridae* while the H2 infectors are classified with the viral family *Autographiviridae* (Figure 2B). These two families are morphologically distinct, with the former having a significantly longer tail than the latter (Li et al., 2022, Bebeacua et al., 2013).

At the genetic level, the 4 *Hafnia* strains also self-classify into two groups (Figure 3A). Genome-wide measurements of relatedness (average nucleotide identity, ANI) suggest that the H1 and H2 *Hafnia* represent distinct species (Figure 3B). One observed difference between them is found in their CRISPR systems; the H1 infectors lack a Cas enzyme cluster and possess a self-targeting spacer, while the H2 infectors have intact Cas genes. Interestingly, both possess spacers that target the Curli prophage region within the H1 genome (Figure 4A). Mauve alignment reveals minimal genetic similarity between this prophage and either of the groups of phages isolated (Figure 4B).

Furthermore, based on Genome BLAST Distance Phylogeny, *Hafnia* JH36 and JH591 are most likely *Hafnia alvei* while JB232 and VRAC originate from a yet uncharacterized species of *Hafnia* (Figure 2B). Therefore, genetic distinction in both bacterial host and phage likely underpins the infection profile observed in phage killing of hosts.

**Establishing phage TS33 for model-host interaction.** Since none of the H2 phages were capable of infecting *Hafnia* JB232, they were excluded from any testing in the community

context. With the focus on JB232-infecting phages, we narrowed it down to phages that were enriched on JB232 only. Since all those phages had an AAI of >98%, had similar plaque morphology, and could be easily used to obtain high titers of  $10^9$  to  $10^{10}$ , we made the assumption that the phages would interact similarly in the community setting. Thus, phage TS33 was selected at random from the JB232-infecting phages.

## **Discussion**

We discussed earlier in this chapter that our understanding of host-phage interactions has been limited by our exclusion of the very community within which these interactions occur. The necessity for more ecologically relevant studies of host-phage interactions has been a topic of recent discussion (Chevallereau et al., 2022). The development of an effective model for the study of host-phage relations within a microbiome is therefore appropriate. Our lab has previously used a small microbial community to scrutinize the molecular mechanisms that underlie bacterial-bacterial interactions within a microbiome (Morin et al., 2018). This study pioneers the addition of a bacteriophage, specifically TS33, to this community to investigate how bacterial-phage interactions are affected by the community and vice versa.

The *Hafnia*-TS33 offers a useful pair to study host-phage interactions for a few reasons. First, both species reside within an already tractable microbial community. Secondly, TS33 is a lytic phage, producing visible clear plaques on *Hafnia*. In other words, it is easy to quantify the interaction taking place, as well as to quantify the bacteriophage. Additionally, TS33 infection of *Hafnia* JB232 produces a high titer of phage after 18 hours of coculture; it is relatively easy to culture enough TS33 for an experiment. Lastly, in this study, we have begun to characterize the TS33 genome via annotation using PATRIC (Gillespie et al., 2011). Although there is more of

the genome left to be characterized, the available annotations give us useful insight into the molecular properties of the bacteriophage.

## Methods

**Media preparation.** All spot titer assays and phage culturing were conducted using liquid or solid LB media at room temperature.

**Bacterial and phage strain selection and preparation.** *Hafnia* JB232 was selected based on its presence in a successful model community previously employed by the lab (Morin et al., 2018). The bacterium was first isolated from a natural rind cheese as previously described (Wolfe et al., 2014). *Hafnia* VRAC, JH36, and JH591 were selected due to their frequent use in cheesemaking at Jasper Hill Farm, VT from which our strains originate.

*Hafnia* is the only bacterium in the model community; thus it was the only genus used to isolate phages from a bloomy rind cheese, and a different batch of the natural rind cheese from which it was originally isolated. The cheese rinds were scraped and homogenized in 2 mL SM buffer (100 mM NaCl, 8 mM MgSO<sub>4</sub>, 50 mM Tris-Cl). The suspension was vortexed vigorously and centrifuged at x13000 rpm, at 4°C. The supernatant was filtered using a 0.45-μM filter (Cytiva). The filtrate was then serially diluted; each dilution was mixed with 200 μL of a late log culture of each *Hafnia* strain and 4.5 mL soft agar (0.05% Bacto-agar, 25% LB), and poured onto solid LB media. After 24 hours, 21 of the resulting plaques were picked and struck out 3 times on solid LB medium on a soft agar lawn of the *Hafnia* strain on which they were enriched. On the third quadrant streak, one plaque from each plate was picked and cultured in liquid LB medium with a colony of *Hafnia* JB232. After 16-18 hours of incubation, the cells were pelleted

and the supernatant was filtered using a 0.45- $\mu$ M filter. This phage lysate was stored at  $-80^{\circ}\text{C}$  with fresh 1XPBS-40% glycerol.

**Testing host range of each bacteriophage.** Soft agar lawns were made from late-log cultures of each strain of *Hafnia* as previously described (See *Methods, Bacterial and phage strain selection and preparation*). Each bacteriophage was serially diluted and spotted onto the soft agar lawns. The presence of plaques on a lawn signified host susceptibility; resistant hosts had no plaque formation.

**gDNA Extraction and Genome Sequencing.** gDNA was extracted from late-log cultures of the 4 *Hafnia* strains and phage lysates using Phenol:Chloroform:Isoamyl alcohol (ph 8) (Sambrook and Russell 2006).

**Bacterial gDNA Extraction.** Cell lysis was conducted by adding lysis buffer (10 mM Tris-Cl pH 8, 100 mM EDTA pH 8, 1% SDS, 10  $\mu\text{g}/\text{mL}$  RNase A, 1 mg/mL Lysozyme) to the pellet, vortexing the tubes at maximum speed and incubating at  $37^{\circ}\text{C}$  for 1 hour. An equal volume of Phenol:Chloroform:Isoamyl alcohol was added to the lysate, after which the tubes were centrifuged at maximum speed for 15 minutes at  $4^{\circ}\text{C}$ . To precipitate the gDNA, 0.1 volume of 10M ammonium acetate and an equal volume of extremely cold isopropanol was added to the aqueous phase (upper layer). After centrifuging for 3 minutes at maximum speed, the pellet was washed with fresh 70% ethanol and resuspended in 25  $\mu\text{L}$  of DNase/RNase-free water overnight.

**Phage gDNA Extraction.** Phage lysates were obtained by co-culturing a scraping from the frozen aliquots of each phage and material from 1 colony of the *Hafnia* strain on which they were enriched. The cells were pelleted, and the supernatant was filtered using a 0.45- $\mu$ M filter.

10% volume of pure chloroform was added to the phage lysate for 30 minutes. The aqueous phase was recovered in an Eppendorf tube, and treated with 1 M MgCl<sub>2</sub> (final concentration = 12.5 μM). The tube was gently mixed. The GE Nuclease Mix (New England Biolabs) was diluted 1:10 and 1 μL was added to each tube. After a 30-minute incubation, 40 μL 0.5M EDTA were added to each tube. 5 μL Proteinase K (New England Biolabs) were added to 1 mL of lysate, followed by 50 μL 10% SDS. The tubes were incubated at 55°C for 1 hour, vortexing every 30 minutes. After the incubation, an equal volume of Phenol:Chloroform:Isoamyl alcohol was added to the lysate, after which the tubes were centrifuged at maximum speed for 15 minutes at 4°C. To precipitate the gDNA, 0.1 volume of 10M ammonium acetate and an equal volume of extremely cold isopropanol was added to the aqueous phase (upper layer). After centrifuging for 3 minutes at maximum speed, the pellet was washed with fresh 70% ethanol and resuspended in 25 μL of DNase/RNase-free water overnight.

**gDNA library preparation and sequencing.** gDNA was quantified using the Qubit dsDNA HS assay kit (Invitrogen). The Illumina iSeq 100 was used to sequence the gDNA from each phage and *Hafnia* VRAC, JH36, and JH591. The genome of *Hafnia* JB232 was sequenced using long reads from Pacific Biosciences and Nanopore technologies, and annotated by IGM Biosciences.

**Comparative Genomics.** For each phage, Illumina reads were assembled into contigs via SPAdes (Bankevich et al., 2012). Initial genomic alignments were done using the Mauve Plugin in Geneious (Darling et al., 2004). Calculations of average nucleotide identity (ANI) for the bacterial genomes were done using the method previously described, and CompareM was used to calculate the average amino acid identity (AAI) (Goris et al., 2007, Rodriguez-R et al., 2016). To visualize genomic similarity, AAI and ANI values were converted into a dendrogram using MegaX; heatmaps were all generated using Python (Kumar et al., 2018). Viral classifications

based on the whole proteome comparisons were performed using the Viral Proteomic Tree (ViPTree) Server (Nishimura et al., 2017). Finally, we used the Type (Strain) Genome Server (TYGS) to perform Genome BLAST Distance Phylogeny (Meier-Kolthoff and Göker, 2019).

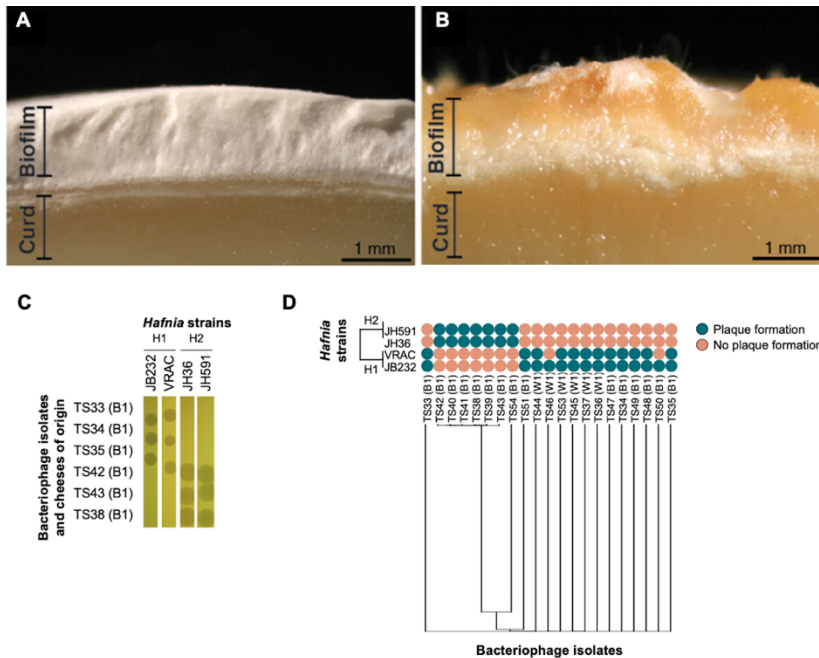


**Figure 2.1. *Hafnia*-phage interactions take place within cheese rinds.** Included in the investigation of *Hafnia*-phage interactions were (A) bloomy rind and (B) washed rind *Hafnia* and phage isolates. (C) Actual plaque formation of cheese phages on lawns of 4 *Hafnia* strains. 5  $\mu$ L of serially diluted suspensions of pure phage were spotted onto each bacterial lawn. (D) Summary of phage plaquing data on *Hafnia* strains. Phages from one washed rind cheese (W1) and one bloomy rind (B1) cheese interact with *Hafnia* in modules: the phages that kill H1 hosts never kill H2 hosts, and vice versa.

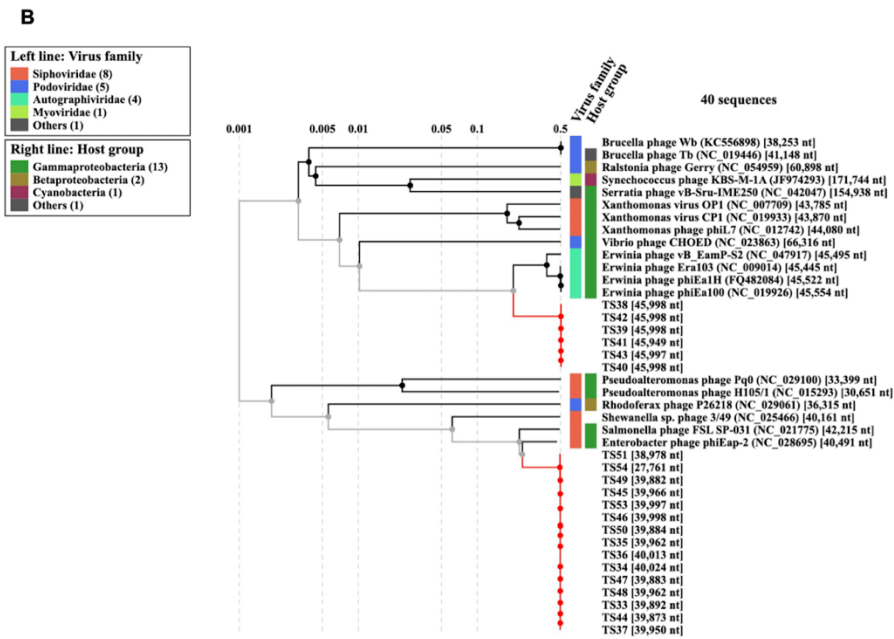
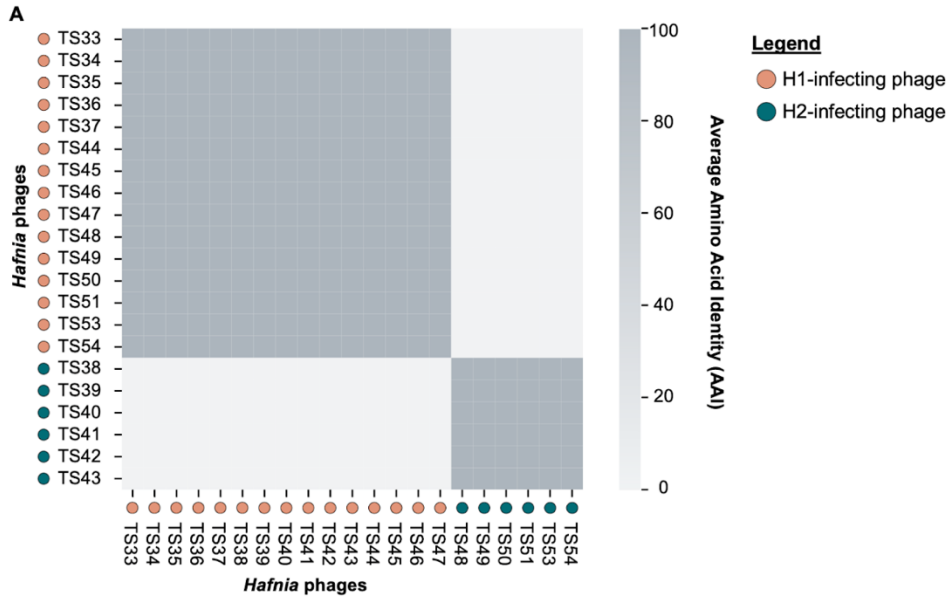


**Figure 2.2. Genetic comparison of *Hafnia* phage genomes.** (a) *Hafnia* phages within each group have a higher pairwise AAI (over 99%) to one another than they do to phages outside that group. (b) *Hafnia* phages cluster into H1 and H2 infectivity groups based on their genomic similarity.

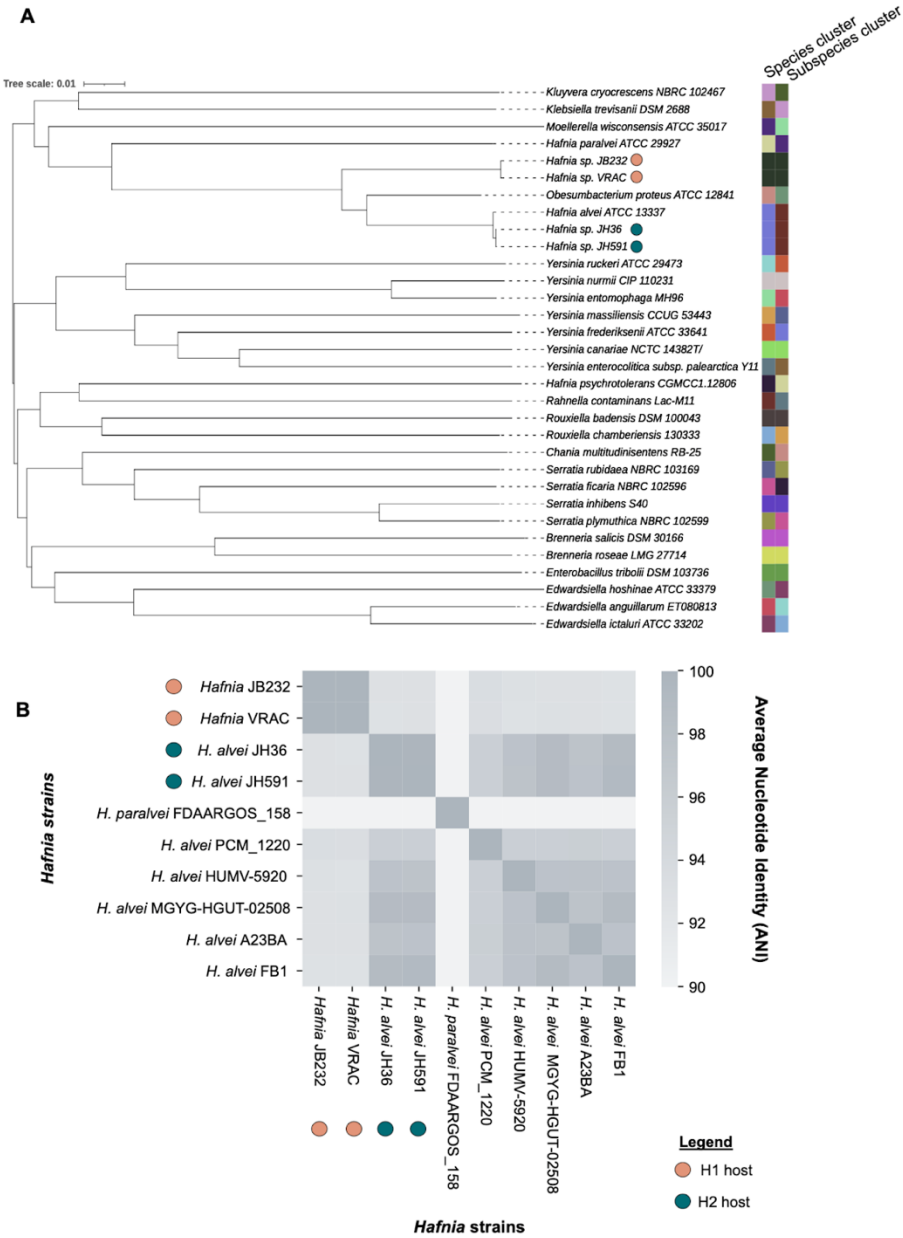


**Figure 2.3. Genetic comparison of *Hafnia* strains.** (A) Cheese *Hafnia* strains within each group meet a higher pairwise ANI (over 95%) to one another than they do to strains outside the group. (B) Cheese *Hafnia* strains cluster into H1 and H2 susceptibility groups based on the alignment of their RNA polymerase beta (*rpoB*) genes. Non-cheese *Hafnia* strains are included for comparison.

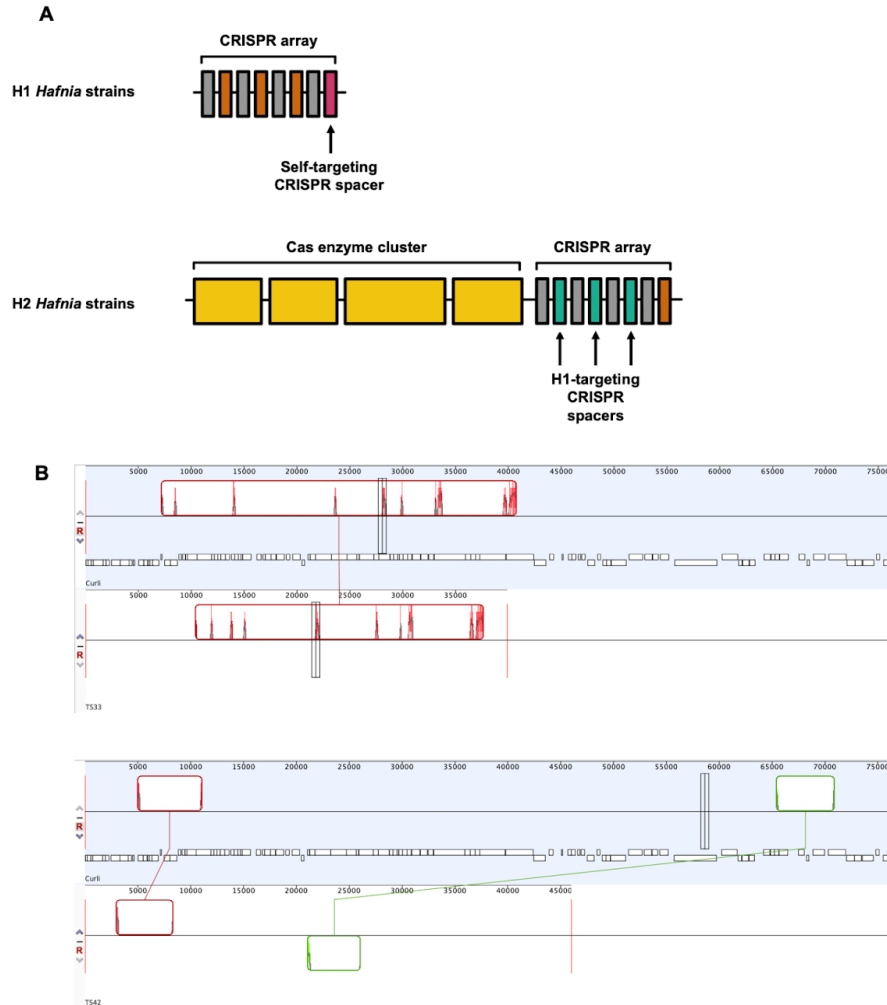


**Figure 2.4. CRISPR systems within *Hafnia* strains used in cheesemaking.** (A) Both H1 and H2 hosts have CRISPR arrays but only H2 hosts encode Cas enzymes. H1 spacers target the Curli prophage region within H1 genomes. Three H2 spacers target the Curli prophage region in the H1 genome. (B) Mauve alignment of Curli prophage and TS33 or TS42 genomes. Red or green vertical lines within boxes indicate regions of genomic similarity. Curli prophage is genetically distinct from TS33 and TS42 genomes.

## CHAPTER 3

### **Chapter 3: O-antigen biosynthesis mediates tripartite interactions between bacteria, phage, and fungi within a simple community**

**Authors: Tara C.J. Spencer<sup>1</sup>, Angel Sarabia<sup>1</sup>, Gary Heussler\*, Steven Villareal<sup>1</sup>, Rachel J. Dutton<sup>1</sup>**

<sup>1</sup>Division of Biological Sciences, Section of Molecular Biology, University of California San Diego, 9500 Gilman Drive, La Jolla, CA, 92093, USA

\*deceased

#### **3.1 Chapter Summary**

Diverse and widespread populations of bacteriophages infect and co-evolve with their bacterial hosts. Although the process of host recognition and infection occurs within microbiomes, the molecular mechanisms underlying host-phage interactions within the context of a community remain poorly studied. The biofilms, or rinds, of cheese contain taxonomically diverse microbial communities that follow reproducible growth patterns and can be manipulated under laboratory conditions. Our lab has previously used a model Brie community to demonstrate specific microbe-microbe interactions occurring within a community. Using this system, we are investigating how host-phage interactions and co-evolution influence other community members, and vice versa. The work outlined here described our efforts to use cheese as a model for studying phage-microbe interactions by identifying and characterizing a tractable host-phage pair co-occurring within this system. We successfully isolated lytic bacteriophage TS33 that kills *Hafnia* sp. JB232, a member of a model Brie community. TS33 is easily propagated in the lab and naturally co-occurs in the cheese with its *Hafnia* host and other

members of the Brie community, rendering it a prime candidate for the study of host-phage interactions. We used Random Barcode Transposon Sequencing (RB-TnSeq) experiments to identify candidate host factors that contribute to TS33 infectivity, many of which are critical to the integrity of the lipopolysaccharide (LPS) layer of the host cell. Notably, disruption of these genes results in decreased susceptibility to infection by phage TS33, while simultaneously exhibiting a significant negative effect on the fitness of *Hafnia* sp. JB232 in the presence of its fungal partners, *Geotrichum candidum* and *Penicillium camemberti*. Therefore, LPS mutations may have pleiotropic effects on the interactions between sp. JB232 and the rest of the Brie community. Ongoing and future studies aim to unearth the molecular mechanisms by which the LPS of sp. JB232 mediates its interactions with its viral and fungal partners.

### **3.2 Developing and using a model system to study host-phage interactions within a community context**

#### **Introduction**

Bacteriophages are the most abundant replicating entities on the planet. Within their microbiome homes, their primary ecological interactions are with their bacterial hosts; they control community composition, host abundance, and host gene expression. As discussed in Chapter 1, our knowledge of the impact of community context on host-phage interactions is quite sparse. The current literature available on the impacts of ecological contexts on host-phage interactions is contradicting. Some studies show that the community may constrain host-phage interactions (Johnke et al., 2017), while others show that the effect of community presence on these dynamics is positive (Mumford & Friman 2016, Gómez & Buckling 2011). Similarly, there are no generalized conclusions drawn about the role of community context on host-phage

coevolution. In some ecosystems, host adaptation to phage predation has been shown to be inhibited by the community (Johnke et al., 2017, Mumford & Friman 2016) while others have negligible impacts on host adaptation (Middleboe et al., 2001) or positive impacts (De Sorti et al., 2019, De Sorti et al., 2017).

However, time is a limiting factor in these studies as many of these experiments take place over 15 generations on average (Blazanin and Turner, 2021). What is more, the microbes under investigation were cultured in an environment that is quite different from their natural habitat. By designing experiments that occur over a realistic ecological timeline, and closely mimic the niche of the microbes, we can paint a clearer picture of the rich biology that takes place within microbiomes. In the study described here, we employ a model community of cheese microbes to investigate the tripartite interactions between phages, bacteria, and fungi.

Our primary approach involves using a high-throughput genetic screen that employs barcoded transposon mutant libraries (RB-TnSeq) to discover microbial interactions within a community context, and investigating how increasing community complexity affects these interactions. TnSeq methods were originally developed to determine the genetic basis of specific phenotypes. Comparisons of gene frequency under various conditions allows us to identify the genes that promote and hinder growth. However, our lab uniquely applied them to the identification of genetic requirements of bacterial hosts in the midst of a community (Opijnen and Camilli 2013). By subjecting the mutant library to various community contexts, we have identified genes and their associated biochemical pathways that are important for the growth of *Escherichia coli* and *Pseudomonas psychrophila* (Morin et al. 2018). Among the important interactions are competition for iron and cross-feeding of amino acids from fungal community

members. We also used this system to demonstrate the reorganization of microbial interactions with increasing community complexity (Morin et al., 2022).

Moreover, RB-TnSeq has been applied to the description of host factors required for phage infection. Adler et al. outline a study in *Salmonella enterica* serovar Typhimurium where a dense library was generated and subjected to phage predation. They successfully identify over 300 genes required for infection by multiple phages, which led to the identification of cross-resistance conferred by the RpoS and RpoN genes (Adler et al. 2021). Similarly, the genetic determinants of phage resistance were also identified in *E. coli* using the same genome scale approach (Mutalik et al. 2020). Among the genes required for phage infection were those associated with synthesis of the Gram-negative lipopolysaccharide (LPS) and nutrient transporters. Additionally, a similar method called INSeq was used by Kortright et al. to verify candidate receptors for various coliphages, among which LPS and transport genes were identified (Kortright et al. 2020).

In this study, we expand our model Brie community by introducing a novel bacteriophage TS33 which naturally lives within the community. In effect, we develop a model within the already existing model community which allows us to study how host-phage interactions occur within a community context. Using a barcoded transposon insertion library in *Hafnia* sp. JB232, we investigate the effects of a community of TS33 and fungal partners, *P. camemberti* and *G. candidum*, on the growth of *Hafnia*, and vice versa. Over the course of the experiment, we observe small negative selective pressure on *Hafnia* origination from the fungi. However, we witness fluctuations in the fitness of *Hafnia* in the presence of TS33 only. Such growth patterns are expected as both the host and phage innovate to preserve their resistance and infectivity,

respectively (Meyer et al. 2012). As a matter of fact, by the end of the experiment, the abundance of *Hafnia* growing with fungi or phage is very similar to that of *Hafnia* growing alone.

What is striking, however, is the stark decrease in *Hafnia* fitness in the presence of both the fungi and the phage. Additionally, DNA sequencing reveals the “unfit” *Hafnia* cells are dominated by mutants in genes required for the synthesis of the cell wall, especially the lipopolysaccharide (LPS). Interestingly, we also identified the LPS as a key genetic determinant of phage resistance in *Hafnia*. Additionally, mutations in these genes offer a negative fitness effect in the presence of the fungi, meaning that these genes are important for resisting negative interactions with fungi. Together, these data highlight the role of LPS in mediating interactions between *Hafnia*, fungi, and phage. Additionally, our experiments highlight the importance of community context in the fitness profile of *Hafnia* interacting with phage TS33, as we are presented with a very different outcome when the fungal partners are excluded.

## Results

**Isolating lytic bacteriophage that kills *Hafnia* sp. JB232.** To establish a model system for studying host-phage interactions within our Brie community, we first isolated a bacteriophage that infects *Hafnia* sp. JB232 from the natural cheese environment of the bacterium. Bacteriophage TS33 was isolated in 2019 from the rind from a different batch of the same cheese that sp. JB232 was first isolated in 2011 (Wolfe et al. 2014). Plaque assays reveal that TS33 infects *Hafnia* sp. JB232, and produces a titer of  $>10^{10}$  pfu/mL following overnight incubation with the host (Figure 1A). The TS33 genome was sequenced using Illumina technologies and subsequently analyzed using the Viral Proteomic Tree (VipTree) server to determine genome-wide similarities to a bacteriophage reference database. These whole genome comparisons predict that TS33 is a member of the viral family *Siphoviridae*. TS33 is most

closely related to *Salmonella* phage FSL SP-031 and *Enterobacter* phage phiEap-2, the latter of which infects multidrug-resistant *Enterobacter aerogenes* (Figure 1B).

**Identifying genetic requirements of *Hafnia* growing under different conditions.** We used a high-throughput genetic approach to determine how different ecological contexts affect the genetic requirements of *Hafnia* sp. JB232. An RB-TnSeq library was developed in sp. JB232 by mating with the *Escherichia coli* Keio\_ML9 RB-TnSeq library from Wetmore et al. 2015. The *Hafnia* library contains 103169 insertion mutations (and thus mutants) in 58869 distinct locations. ~88% of the protein-coding genes are disrupted, with insertions being in only 10-90% region of those genes (Figure S1B). Moreover, for each gene represented in the library, there were on average 25.6 different insertion mutants generated.

For this series of experiments, I grew a pooled transposon mutant library of *Hafnia* sp. JB232 on an *in vitro* cheese medium, either alone or in the presence of the Brie community members for 3 days (Figure 2A-B). Additionally, each experimental condition was performed with or without phage added. For each day of the experiment, cells and phage particles were harvested, diluted, and plated for counting.

To determine the effect of ecological context on the genes required for *Hafnia* growth, the pooled transposon mutant library was inoculated on an *in vitro* cheese medium either alone or in the presence of the fungal partners from the Brie community, *Geotrichum candidum* and *Penicillium camemberti* in a 1:1 ratio. Additionally, each experimental condition was performed with or without phage TS33 (MOI=0.001). On each day of the experiment, cells, spores and phage particles were harvested, diluted, and plated for counting (Figure 2).

*Geotrichum* grows steadily over 3 days, attaining levels that are minimally impacted by the presence of bacteria phage, bacteria only or *P. camemberti* (Figure 2B). Similarly, *Hafnia*

and TS33 growth levels do not appear to be vastly impacted by the presence of any or both fungi (Figure 2A). However, in the presence of the phage, the number of *Hafnia* colony-forming units (cfus) decrease on day 1, recover on day 2, and decline again on day 3. Moreover, *Hafnia* growth conditions that included both TS33 and either fungus or both fungi exhibited complete extinction of *Hafnia* from the community by day 3 (Figure 2A). These data suggest that when both phage and fungi are present, *Hafnia* fails to recover its population levels. Moreover, our data show that TS33 density is not amenable to most conditions, except when TS33 is interacting with *Hafnia* in the presence of both *G. candidum* and *P. camemberti*. We observe that the community presence significantly decreases in the amount of phage particles ( $p < 0.005$ ) after three days of growth. All in all, the presence of the community negatively affects the growth of both *Hafnia* and TS33 (Figure 2A).

To determine the fitness of different *Hafnia* mutants, we investigated the composition of the library under each condition on day 3. DNA was extracted from the day 3 samples, and the RB-TnSeq barcodes were amplified using PCR and sequenced. For each replicate in each condition, the number of reads per barcode, i.e. the abundance of each barcode, was used to assign a fitness value to each disrupted gene in the mutant library (Figure 3A, Figure S2). These values were then statistically analyzed to obtain a t-score for each gene represented in the library.

Of the 4021 protein-coding genes represented in the library, we successfully obtained fitness values and moderate t-scores for 3863 (96.07%). We employed t-score statistics to filter out genes that lacked a strong fitness effect, that is, genes whose fitness values are below the limit of detection. In our dataset, this was approximately 96% of all genes (3713/3863). For each gene, the assigned moderate t-score measures the probability that the fitness value will be different from 0 (below the limit of detection). In every condition, most genes with a t-score  $< 3$

had a fitness value that was undetectable. In other words, genes with an absolute t-score of  $\geq 3$  had strong fitness effects. There were 150 genes with strong fitness effects in any condition, of which 4 were conserved across all 4 conditions (Figure 3B).

Next, we compared the gene functions assigned to these 150 genes among the different ecological contexts of *Hafnia* growth in order to identify the molecular pathways enriched therein. To this end, each gene with a strong fitness effect was annotated using the KEGG Orthology and Links Annotation (KOALA) BLAST and mapped to the KEGG BRITE database (Kanehisa et al. 2016, Figure 3C). For each condition, we calculated the percent of the total annotations represented by each KEGG annotation, and then looked specifically for groups that were abundant in all 4 conditions of growth. Genes classified under “Protein families: metabolism” and “Glycan biosynthesis and metabolism” were enriched in all 4 conditions. It is important to state that 52.9% of the genes classified under “Protein families: metabolism” received the annotation “Glycan biosynthesis and metabolism” or the sub-annotation “Lipopolysaccharide biosynthesis proteins”. Moreover, the glycan biosynthesis and metabolism genes are all involved in lipopolysaccharide (LPS) biosynthesis. The LPS is a glycolipid that is comprised of three parts - lipid A, the core polysaccharide, and the O-antigen and is the most outward-facing part of the structure. The LPS is well documented as a critical cell structure for combatting attacks from bacteriophages, other bacteria, and chemicals (Cai et al. 2019, West et al. 2005). Specifically, it is a common adsorption site for diverse bacteriophages (Letarov and Kulikov 2017, Silva et al. 2016). Here, we see that the LPS genes are enriched in some way under all conditions of growth.

To determine the specific impacts of these genes in each condition, we investigated the fitness effects of each gene associated with glycan/LPS biosynthesis and metabolism. Positive

fitness effects are assigned to mutants whose abundance at T=3 exceeds their abundance T=0, as well as the abundance of all other mutants in the library under this growth condition. Conversely, the mutants who decrease in abundance experience a negative fitness effect. The LPS biosynthesis genes were primarily annotated as *rfa* genes (known players in LPS biosynthesis in *E. coli*, Klena et al., 1992) and glycosyltransferases predicted to be involved in cell wall biosynthesis (Figure 3A).

Insertions in the *rfaL* gene, which synthesizes the O-antigen ligase, exhibit positive fitness effects in all conditions containing phage, and negative fitness effects in the presence of fungi only (Figure 3A, Figure 3D). These fitness effects were stronger than those observed when *Hafnia* grows alone. Interestingly, disruption of the *rfaZ* (KDO-transferase) gene has a relatively small positive effect on the fitness of *Hafnia* growing with fungi; however, this effect is three times greater when *Hafnia* grows with phage TS33 and is seven times greater when *Hafnia* grows in the community (Figure 3A, Figure 3D). Another operon encoding predicted glycosyltransferases that contribute to cell wall biosynthesis follows a similar pattern; overall, we observe that mutations in any genes from this operon have negative fitness effects on *Hafnia* growing with fungi, and positive fitness effects during growth with phage or the whole community. In other words, in the presence of TS33, disrupting LPS biosynthesis appears to provide a fitness benefit to *Hafnia* but may offer a fitness cost in the presence of the fungi.

It is worth noting that the positive fitness effects that we observe in these genes when *Hafnia* is growing with the community may be attributed to strong selection for them by the phage. Subsequently, they succumb to potentially negative interactions with the fungi, evidenced by the stark decrease in the growth of *Hafnia* in the community context compared to all other

conditions. Thus, we hypothesized that some genes involved in LPS synthesis might have pleiotropic effects in *Hafnia*.

**Determining the role of LPS in host-virus-fungus interactions.** To test our hypothesis, we used a high titer of phage to select for phage-resistant *Hafnia* mutants (Figure 4A). We successfully isolated mutants only in genes involved in LPS and specifically, O-antigen biosynthesis: *rfaL*, *rfaH*, *manC* (mannose-1-phosphate guanylyltransferase), and a predicted O-antigen polymerase gene. RfaH is a transcriptional antiterminator that regulates the expression of genes involved in LPS biosynthesis, while ManC (RfbM in *Salmonella*) is involved in the synthesis of the growing O-antigen.

We hypothesized that the susceptible insertion mutants within the *Hafnia* library growing with TS33 experience high levels of phage predation, resulting in the community being dominated by TS33-resistant mutants and accounting for the spike in *Hafnia* counts on Day 2. However, eventually, the *Hafnia* counts recover, possibly due to the emergence of counter-resistant mutations in TS33. However, in the presence of either fungus or both fungi, the TS33-resistant mutants experience a negative fitness, resulting in their decrease in growth in any ecological context containing fungi (Meyer et al. 2012, Figure 2A).

To directly test this hypothesis, we aimed to determine whether TS33-resistant mutants with disrupted LPS genes experience a fitness deficit in the presence of both fungi. We subjected the *Hafnia* library to high titers of TS33 for 24 hours in liquid LB. The remaining viable cells were plated on solid LB media and the emergent colonies were picked and struck three times to purify the strains. Phage TS33 was diluted and titered on top agar lawns of each mutant. In total, we isolated and sequenced the barcodes of 50 mutants, each displaying decreased or no susceptibility to the TS33 lysate compared to the wild-type (Supplementary Table 3.1).

Sequencing of the mutant barcodes revealed disruptions in the genes associated with biosynthesis of the cell wall, especially of the LPS. From the 50 mutants, we selected 5 that were represented in our RB-TnSeq results in at least one of the 3 experimental conditions: 1 in *manC*, 1 in *rfaL*, 1 in *rfaH*, which transcriptionally controls the expression of other *rfa* (LPS-synthesizing) genes, and 2 in *wzy*, which encodes an O-antigen polymerase (Iguchi et al. 2015) (Figure 4A). The mutant and wild-type *Hafnia* cells were then inoculated on *in vitro* cheese medium with or without the fungal community members. After 3 days, the cells were harvested and quantified. For each *Hafnia* strain plated, we compared the number of cfus after growth with fungi to that after growth alone (Figure 4B, Figure S3A).

The  $\Delta wzy$  mutants were completely resistant to infection by phage TS33, while the  $\Delta manC$ ,  $\Delta rfaL$ , and  $\Delta rfaH$  mutants exhibited drastic reductions in their susceptibility. From these results, we can observe a fitness benefit to the *Hafnia* cells by the disruption of genes involved in O-antigen synthesis, with the strongest benefit coming from the interruption of the O-antigen polymerase gene (Figure 4A, Figure S3B). Interestingly, in the presence of the fungi, the  $\Delta rfaL$ ,  $\Delta rfaH$  and  $\Delta wzy$  mutants experience a significant decrease in growth, compared to the wild-type (Figure 4B), strongly suggesting a role played by the O-antigen in the modulation of interactions between *Hafnia* and its viral and fungal environment. This fitness defect is not observed in the  $\Delta manC$  mutant, although *manC* is also involved in O-antigen synthesis (Thomson et al. 2003). The failure of the disruption of *manC* to negatively affect *Hafnia* fitness in the presence of the fungi suggests that these specific sugar residues are not required for *Hafnia*-fungi interactions.

## Discussion

Most studies of bacteria-phage interactions completely exclude the natural community wherein the microbes exist naturally. In this study, we used *Hafnia* sp. JB232 interactions with

phage TS33 as a model to uncover the principles of community impact on host-phage interactions. Under each condition of growth, we quantified the number of bacterial cells to understand the effects of different combinations of community members on *Hafnia* growth. Moreover, using a high-throughput genetic screen, we were able to further investigate these growth effects by studying the fitness landscape of the *Hafnia* cells in each growth condition. Our analyses reveal that fungi have minimal effects on the overall growth of the *Hafnia* mutants, while the phage can lead to fluctuations in *Hafnia* growth that eventually the bacteria recover from. During the time period of our experiment, neither the phage nor fungi alone elicited as drastic a depletion in the final counts of *Hafnia*, as both of them did together. In other words, neither group of community partners is sufficient to produce a strong negative outcome on *Hafnia* growth; both are required for extinction of *Hafnia*.

Similar and contradicting observations have been made by other scientists. In a study of wastewater microbial ecology, Johnke et al. unearthed suppressive effects of a microbial community on *Klebsiella* sp. (Johnke et al., 2017). Under phage selective pressures, the bacterium experiences more severe impacts on its growth. In the same study, they also show that the presence of some other specific community members contributes to the sustained growth of *Klebsiella*. Conversely, *P. fluorescens* and *P. aeruginosa* both benefitted from a community presence amidst phage predation (Gómez & Buckling 2011, Mumford & Friman 2016). While our results most closely support those projected by Johnke et al., it is probable that the community effects are dependent on community composition. Our studies involved the use of fungi, *P. camemberti* and *G. candidum*, which are known to have negative interactions with other microbes. *P. camemberti* produces a beta lactam antibiotic in the presence of *E. coli* (Pierce et al. 2021). Moreover, *G. candidum* is believed to exert oxidative stress on *E. coli* (Morin et al.

2018). In the presence of the fungus, *E. coli* depends heavily on genes such as *acrA* and *acrB* that enable it to resist oxidative stress. Moreover, in the presence of the community, these genetic requirements are alleviated, suggesting that activity from one of the community members is either preventing oxidative stress or empowering *E. coli* to deal with it. It is possible that these molecular products of both fungi produce a negative effect on *Hafnia* mutants resistant to phage infection. To further understand the relationship between community presence and growth of focal bacteria, it is essential to investigate the molecular mechanisms that underlie their interactions.

Our study revealed a unique role of the LPS, specifically the O-antigen, in *Hafnia*'s interactions with its community. The LPS is a major component of the defense mechanism of Gram-negative bacteria, as it protects them from chemical attacks by other microbes and the environment. The intact LPS is often exploited by phage during attachment to the host (Letarov and Kulikov 2017). In fact, the O-antigen has been shown to be a specific target of several bacteriophages (Broeker and Barbirz 2017). Additionally, phages and antimicrobials are known to negatively affect bacterial cells with compromised LPS (Ebbensgaard et al. 2018, Burmeister et al. 2020). Burmeister et al. demonstrate that LPS mutations confer phage resistance but restore antibiotic susceptibility (Burmeister et al. 2020). We observe that *Hafnia* LPS mutants develop resistance to TS33 infectivity while experiencing growth deficits in the presence of the fungi. In light of the negative interactions that these fungi are known to have with other microbes, it is possible that the antibiotic/oxidative stress that they apply accounts for the growth defect in LPS mutants growing under these conditions. In other words, genes controlling LPS biosynthesis may have pleiotropic effects in *Hafnia*, and lead to trade-offs with evolutionary consequences for *Hafnia* growing in a community of fungi and phage.

There is additional evidence that the negative effects of antibiotics on LPS-deficient cells may be genotype-specific. In a study by McGee et al., 3 of 4 LPS mutants under study were resistant to both phage and antibiotics of various classes (McGee et al., 2023). They observe that *rfaH* and *yciM* (controlling synthesis of Lipid A; Sunayana and Reddy, 2013) mutants are phage and antibiotic-resistant; the phage-antibiotic resistance trade-off was observed only in the *rfaP* (facilitating synthesis of the core oligosaccharide) mutant. While we were not able to isolate an *rfaP* mutant for our experiments, our findings do suggest that all LPS mutations may not provide a trade-off within a community context, as the *ΔmanC* mutant did not experience a growth deficit in the presence of the fungi. Combining our results with those of McGee et al., it is plausible that some Lipid A and the O-Antigen mutations are implicated in increased susceptibility to antibiotics.

Furthermore, our unique approach to the study of host-phage interactions underscores the critical importance of considering the community in these investigations. Using *Hafnia* as a model, we show that the ecological context can affect the growth outcome of bacteria. The outcome of *Hafnia*-TS33 interactions is more positive when the fungi are absent. Additionally, the fungi have a negative effect on the fitness of *Hafnia* that is not observed in the growth condition with the fungi. The phage also experienced density suppression mediated by the fungi. These results are similar to what is seen in wastewater microbiomes, where protists negatively impact host-phage interactions. Therefore, including all members of the community in our study allowed us to observe the dependence of *Hafnia*-phage interactions on both fungi.

Altogether, our findings shed light on the unique contributions of community members to bacteria-phage interactions, and thus, reinforce the need to consider the microbiome in studies of the biology of bacteria and phages. Additionally, through this study, we have just begun to

understand the role of the LPS in mediating host-phage interactions within a community. Moreover, by establishing a model host-phage interaction within a community context, we have provided a starting point for full comprehension of the dynamic relationships that exist among fungi, phage, and bacteria.

## **Methods**

**Media preparation.** Community growth assays were performed using 10% cheese curd agar at pH 7 (10% freeze-dried Bayley Hazen Blue cheese curd (Jasper Hill Farm, VT), 3% NaCl, 0.5% xanthan gum, and 1.7% agar); 10M NaOH was used to buffer the pH from 5.5 to 7 (Wolfe et al. 2014). All growth assays and inoculations were performed at room temperature.

**Bacterial, fungal, and phage strain selection and preparation.** All bacterial and fungal isolates were obtained from a natural rind cheese as previously described (Wolfe et al. 2014). The community was selected based on its success as a model in a prior study conducted in the lab (Morin et al. 2018).

As *Hafnia* sp. JB232 is the only bacterium in the model community, it was used to isolate phages from a different batch of the natural rind cheese from which it was originally isolated. The cheese rind was scraped and homogenized in SM buffer (100 mM NaCl, 8 mM MgSO<sub>4</sub>, 50 mM Tris-Cl). The suspension was vortexed vigorously and centrifuged at maximum speed, at 4°C. The supernatant was filtered using a 0.45-μM filter. The filtrate was then serially diluted; each dilution was mixed with 200 μL of a late log culture of *Hafnia* sp. JB232 and 4.5 mL soft agar (0.05% Bacto-agar, 25% LB agar), and poured onto solid LB media. After 24 hours, the resulting plaques were picked and struck out 3 times on solid LB medium with *Hafnia* sp. JB232. On the third quadrant streak, one plaque was picked and cultured in liquid LB medium with a

colony of *Hafnia* sp. JB232. After 16-18 hours of incubation, the cells were pelleted and the supernatant was filtered using a 0.45- $\mu$ M filter. This phage lysate was stored at  $-80^{\circ}\text{C}$  with fresh 1XPBS-40% glycerol.

To prepare stocks of *P. camemberti* and *G. candidum*, spores were obtained from Danisco and resuspended in 1XPBS-Tween0.05%. Spore stocks of equal volume were aliquotted with fresh 1XPBS-40% glycerol and stored at  $-80^{\circ}\text{C}$ . To quantify the stocks, aliquots were frozen for 48 hours, after which they were thawed and plated on solid LB medium. For each fungal strain, we calculated the number of cfus per milliliter of strain stock.

**Transposon mutant library construction in *Hafnia* sp. JB232.** *Hafnia* sp. JB232 was mutagenized by conjugation with *E. coli* strain APA766 (donor WM3064 which carries the pKMW7 Tn5 vector library containing 20 bp barcodes) (Wetmore et al. 2015). In pilot experiments, improved conjugation efficiencies were observed when the donor and recipient strains were at the mid-log phase prior to conjugation. The APA766 donor strain was grown in LB-kanamycin:diaminopimelic acid (DAP) (1 mL frozen stock into 99 mL of LB with 50  $\mu\text{g}/\text{mL}$  kanamycin and 60  $\mu\text{g}/\text{mL}$  DAP) at 37 deg C at 200 rpm until the culture reached mid-log phase. *H. alvei* sp. JB232 was grown in LB at 30 deg C at 200 rpm until the culture reached the mid-log phase. *E. coli* donor cells were pelleted and washed twice with 100 mL of LB without antibiotic. Donor and recipient cells were mixed at a 1:1 cell ratio based on OD600 measurements, pelleted, and resuspended in 100  $\mu\text{L}$ . 40  $\mu\text{L}$  of the mix was plated on a nitrocellulose filter on an LB plate containing 60  $\mu\text{g}/\text{mL}$  DAP. Conjugation took place at 30 deg C overnight. 8 conjugations were performed. The conjugations were each resuspended in 2 mL of LB broth and then 100  $\mu\text{L}$  was plated on an LB:kanamycin (50  $\mu\text{g}/\text{mL}$ ) agar plate. This was done for a total of 120 selection plates. Plates were left at room temperature until single colonies formed (about 3 days). The

resulting transconjugants were scraped into LB from the selection plates and pooled together. The resulting pool was mixed well and then diluted back to an OD600 of 0.2 in liquid LB:kanamycin (50 ug/mL). The pool was then grown to mid-log phase, and two 5 mL samples were taken and pelleted. Cell pellets were frozen at -80 deg C for later library characterization. Sterile glycerol was then added to a final concentration of 15%. 1-mL glycerol stocks were stored at -80 deg C. The final library was estimated to contain ~160,000 mutants.

***In vitro* community experiment using RB-TnSeq library in *Hafnia* sp. JB232.**

**Library pre-culture.** The *Hafnia* sp. JB232 transposon library was thawed on ice, and cultured in liquid LB with kanamycin (1 µg/mL) to the mid-log phase. 5 mL of the preculture was stored at -80°C to be used as the T0 reference in the fitness analysis.

**Inoculations.** The remaining cells and thawed spores were pelleted and washed in 1XPBS/Tween before inoculation. Respective to the condition of growth,  $2.4 \times 10^5$  cfus of *Hafnia*,  $3.37 \times 10^5$  cfus *P. camemberti*,  $3.59 \times 10^5$  cfus *G. candidum*, and  $4.18 \times 10^3$  pfus TS33 were inoculated on CCA plates using sterile glass beads.

**Harvest.** At T=24h, 48h, and 72h, cells, spores, and phage particles were harvested from the fitness assays. For each harvest, CCA plates were flooded with 2-3 mL of 1XPBS-Tween0.05% and cells were gently scraped off. Cells and/or spores were pelleted, and the pellets were washed twice. In conditions containing phage, the supernatants generated after each wash were combined. Before quantification, cells and supernatants from each fitness assay were aliquoted and stored in 1XPBS-40% glycerol at -80°C before quantification. The remainder was stored at -80°C without glycerol for DNA extraction.

**Growth quantification.** Cells/spores in frozen stocks were pelleted by centrifugation and washed with 1XPBS-Tween0.05%. The cells were resuspended in 200 µL 1XPBS-Tween0.05%,

serially diluted, and spread evenly on solid LB media using glass beads. Frozen aliquots of phage were thawed, serially diluted, and titered on a soft agar lawn of *Hafnia* (as described in *Methods, Bacterial, fungal, and phage strain selection and preparation*). The number of colonies and plaques were used to calculate the number of colony-forming and plaque-forming units, respectively, in 1 milliliter of harvested material. Subsequently, we calculated the total number of cfus and pfus harvested. These values were analyzed for statistical significance using R version 4.2.2.

**gDNA Extraction.** From each fitness assay, gDNA was extracted using Phenol:Chloroform:Isoamyl alcohol (ph 8). Cell lysis was conducted by adding a homemade lysis buffer (10 mM Tris-Cl pH 8, 100 mM EDTA pH 8, 1% SDS, 10 µg/mL RNase A, 1 mg/mL Lysozyme) to the pellet, vortexing the tubes at maximum speed and incubating at 37°C for 1 hour. An equal volume of Phenol:Chloroform:Isoamyl alcohol was added to the lysate, after which the tubes were centrifuged at maximum speed for 15 minutes at 4°C. To precipitate the gDNA, 0.1 volume of 10M ammonium acetate and an equal volume of extremely cold isopropanol was added to the aqueous phase (upper layer). After centrifuging for 3 minutes at maximum speed, the pellet was washed with fresh 70% ethanol and resuspended in 25 µL of DNase/RNase-free water overnight.

**Barcode Amplification and Sequencing.** After resuspension, the DNA was quantified via Qubit dsDNA HS assay kit (Invitrogen). Subsequently, we used the BarSeq PCR protocol devised by Wetmore et al. 2015 to amplify only the barcoded region of the transposons. The PCR reaction and program used were also previously reported by Morin et al. 2018. In total, we performed 13 PCRs (T0 sample and 12 harvest samples) involving 13 different multiplexing indexes. 10 µL of each PCR product was pooled, after which the entire pool was purified using the Qiagen

MinElute purification kit and quantified via Qubit dsDNA HS assay kit (Invitrogen) and sequenced at Novogene on 1 HiSeq PE 150 lane (6 bp, i7 single index, Illumina). The output of the lane was 375 million reads.

**RB-TnSeq data processing.** To calculate fitness values for each gene represented in the library, the barcode reads were processed using the Perl script BarSeqTest.pl from Wetmore et al. 2015, and selection criteria previously reported by Morin et al. 2018. Gene fitness values were calculated at T = 72 hr (Day 3) in all four growth conditions. Genes with significant fitness values were assigned based on a corresponding absolute t-score of 3 or more.

**Selection and isolation of TS33-resistant mutants for fitness assay.** TS33-resistant mutants were isolated from the RB-TnSeq library in two ways.

First, the library was pre-cultured to the late-log phase in liquid LB medium with kanamycin (1  $\mu\text{g}/\text{mL}$ ) and  $1.5 \times 10^8$  pfus TS33. The cells were pelleted, washed twice, and resuspended in 1XPBS-Tween0.05%. The cells were then diluted and each dilution was plated on solid LB media using sterile glass beads. 8 colonies were picked and struck twice on solid LB media. Titer assays of TS33 on soft agar lawns on these strains showed that they are completely resistant to TS33 infection. Whole genome sequencing was conducted at SeqCenter, LLC. Two *wzy* mutants were selected from this set.

Second, the library was pre-cultured to the late-log phase in liquid LB medium with  $1.5 \times 10^8$  pfus TS33 and no kanamycin. The cells were pelleted, washed twice, and resuspended in 1XPBS-Tween0.05%. The cells were then diluted and each dilution was plated on solid LB media using sterile glass beads. 42 colonies were picked and struck twice on solid LB media. Titer assays of TS33 on soft agar lawns on these strains showed varying levels of resistance across the mutants, with some being completely resistant and others showing significantly

decreased susceptibility to TS33 infection. Barcode amplification was conducted as previously described (see *Methods, Barcode Amplification and Sequencing*). Whole genome sequencing was conducted at SeqCenter, LLC on three mutants ( $\Delta rfaL$ ,  $\Delta rfaH$ ,  $\Delta manC$ ).

***In vitro* fitness assay using insertion mutants in *Hafnia* sp. JB232.**

**Inoculation.** The 5 selected mutant strains and the WT *Hafnia* sp. JB232 were pre-cultured to late-log phase in liquid LB medium. The cells were pelleted by centrifugation and washed twice with and resuspended in 1XPBS-Tween0.05%. Frozen stocks of *G. candidum* and *P. camemberti* were washed twice with and resuspended in 1XPBS-Tween0.05%. For each strain,  $\sim 1.08 \times 10^8$  cfus on average were plated on CCA medium, with or without both fungi ( $3.82 \times 10^6$  cfus of *G. candidum* and  $9.82 \times 10^5$  cfus *P. camemberti* were plated).

**Harvest.** After 72 hours, the cells and spores were harvested using 1XPBS-Tween0.05% as previously described (See *Methods, Harvest*).

**Quantification of growth.** The harvested cells and spores were diluted in 1XPBS-Tween0.05% and plated on solid LB medium. *Hafnia* colonies were counted and the number of cfus harvested was calculated for each mutant under each condition of growth (alone or with fungi). These values were analyzed for statistical significance using R version 4.2.2.

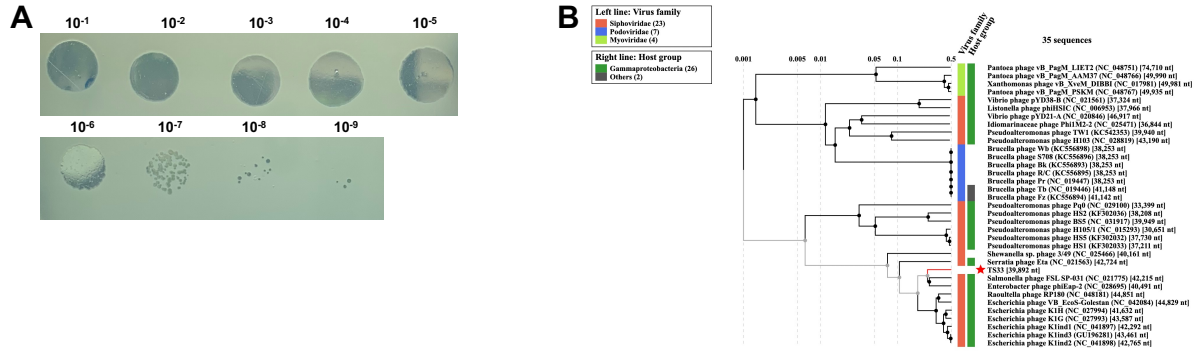


**Figure 3.1. Novel lytic JB232-infecting bacteriophage TS33 is phylogenetically related to members of virus family Siphoviridae.** (A) Actual plaquing of JB232 phage on *Hafnia* lawn. 3  $\mu$ L of serially diluted suspensions of pure phage lysates were spotted onto a JB232 lawn. (B) Proteomic tree showing the predicted phylogenetic classification of TS33 among Siphoviridae. Phylogeny was determined based on whole genome comparison of the TS33 proteome to the proteomes of well-characterized bacteriophages using the Viral Proteomic Tree (ViPTree) Server.

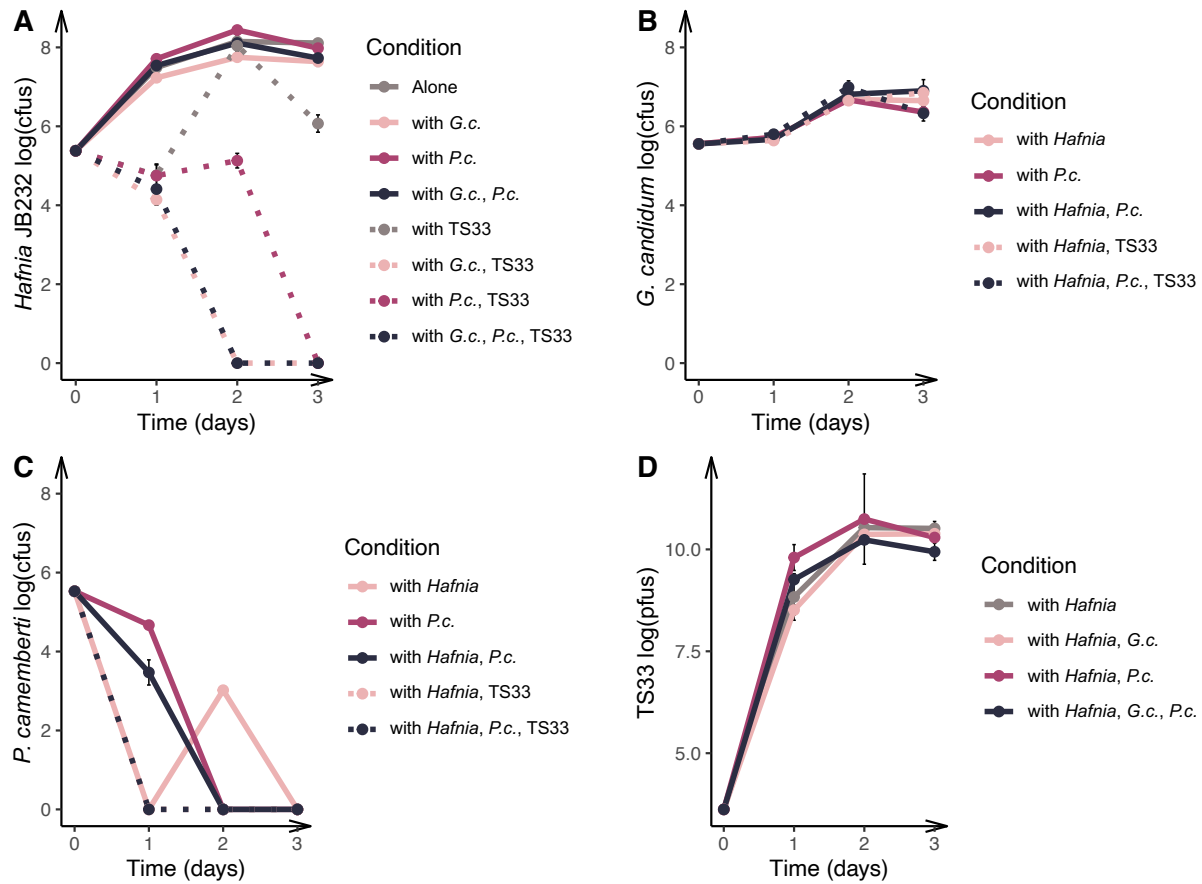


**Figure 3.2. *Hafnia* library growth is inhibited in the presence of a community of fungi and bacteriophages.** The *Hafnia* sp. JB232 library was grown alone, and with phage and/or fungi on *in vitro* cheese medium for three days. The harvested cells (A), spores (B,C) and phage particles (D) were plated on each day and quantified using the total number of cfus and pfus respectively.

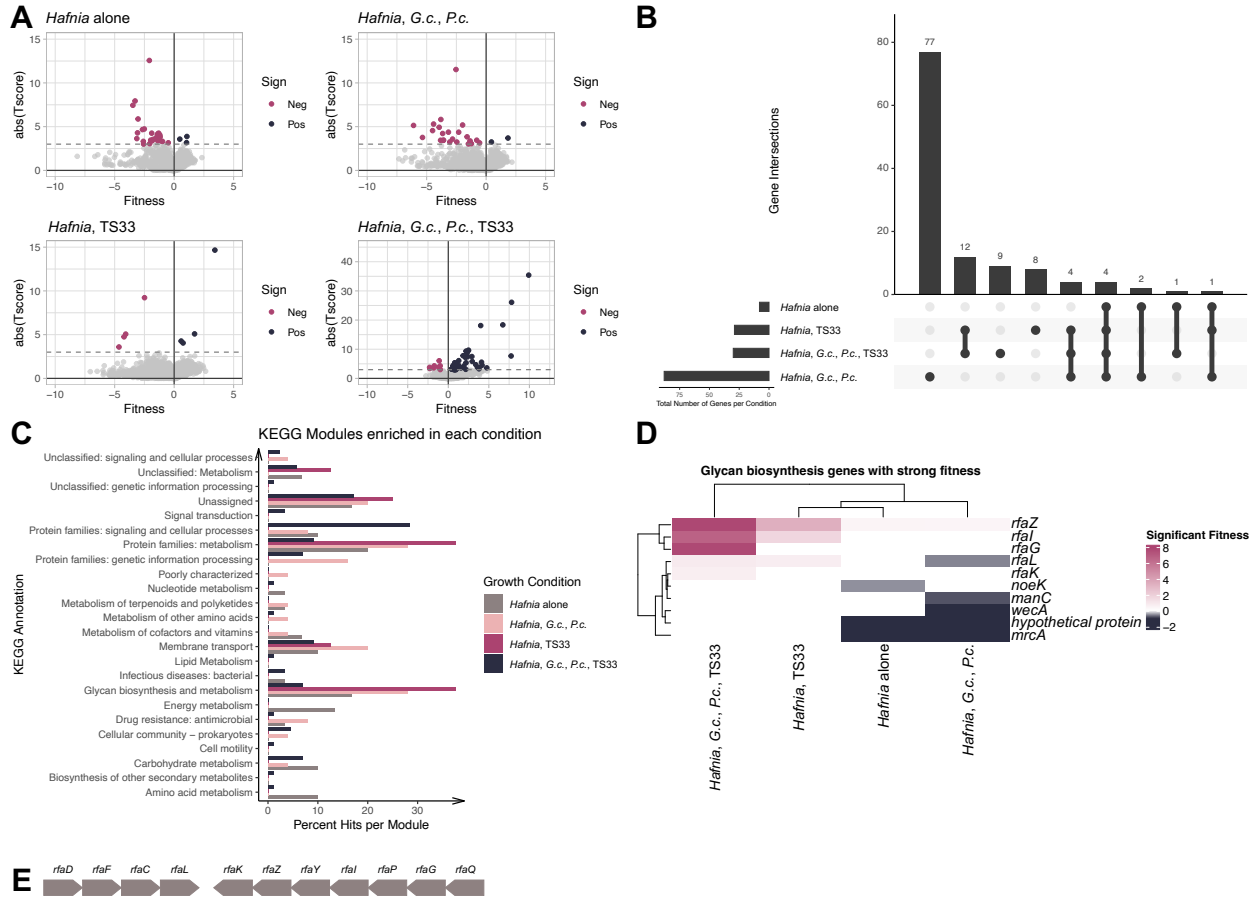


**Figure 3.3. Mutations in genes controlling O-antigen synthesis and ligation may exhibit pleiotropic effects.** (A) The barcodes of the *Hafnia* library plated under various growth conditions were amplified and sequenced. The original RB-TnSeq bioinformatic pipeline developed by Wetmore et al. (2015) was used to quantify each barcode and determine the abundance of each mutant in each gene represented in the library. The sum of the abundances of each mutant for each gene was used to assign a fitness value to each gene. Mutations with a significant negative and positive fitness effect are represented in burgundy and blue respectively. (B) The number of genes unique to and shared by the 4 growth conditions were determined using the UpSet R function developed by Conway et al. (2017). (C) The KEGG Mapper was used to identify gene pathways enriched under each condition. (D) ComplexHeatMap in R was used to compare the enriched genes under each condition. (E) Schematic representation of *rfa* operon in *Hafnia* JB232 Wildtype. Adapted from Pagnout et al. (2019).

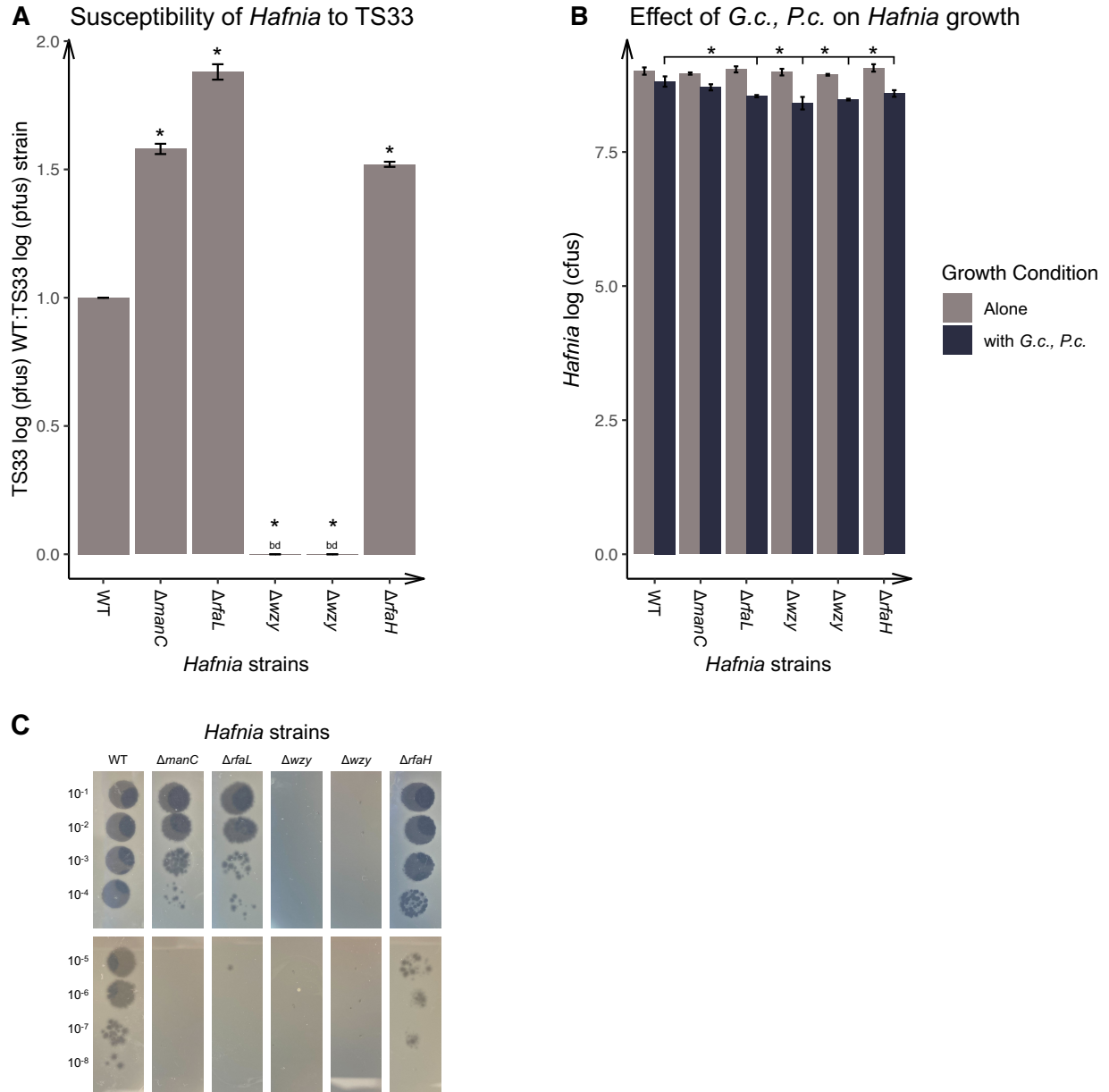
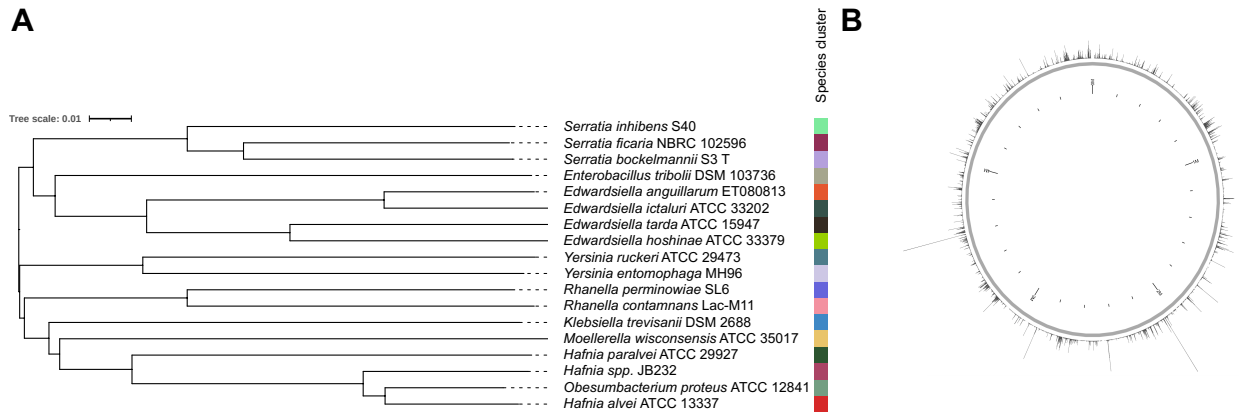
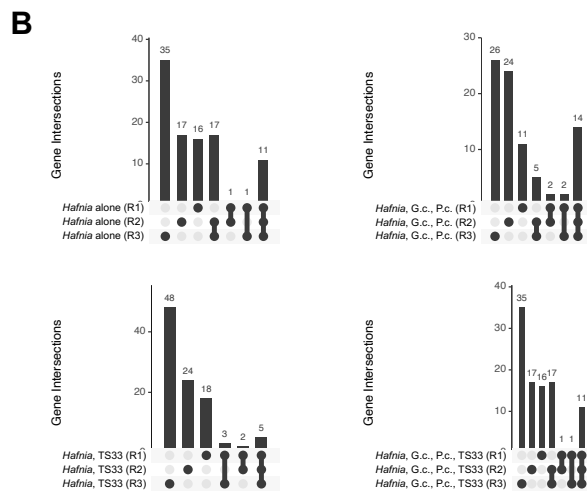
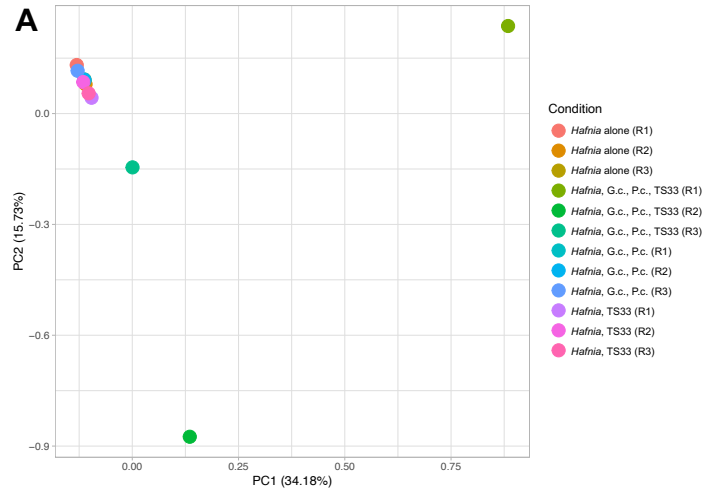


**Figure 3.4. LPS mutations increase *Hafnia* sp. JB232 resistance to TS33 infection but decrease bacterial growth in the presence of the fungi.** (A) Comparing phage infectivity of WT and mutant strains. Phage infectivity is measured by the number of TS33 phage particles (shown here as the number of plaque forming units/pfus) produced following infection on a soft agar lawn of each bacterial strain. (B) Effects of fungi on growth of *Hafnia* strains over 3 days, measured in the number of viable bacterial cells (represented here in colony forming units (cfus)). (C) Images of phage plaquing on various *Hafnia* mutants.

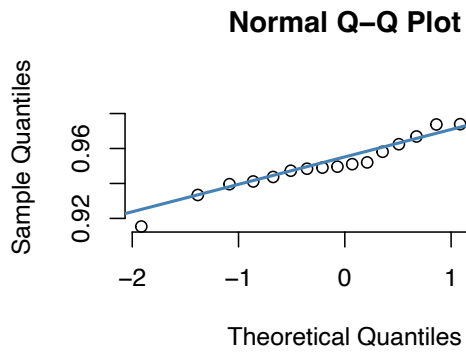


**Supplementary Figure 3.1. Genomic analysis and manipulation of cheese bacterial strain JB232.** (A) Genome Based Distance Phylogeny (GBDP) tree based on genome data reveals that JB232 forms a unique species cluster within the genus *Hafnia*. Phylogeny was determined using the Type (Strain) Genome Server (TYGS) and the tree was visualized using Interactive Tree of Life (iTOL). (B) Insertion map of JB232 genome library. The RB-TnSeq library was constructed in the laboratory via conjugation with *Escherichia coli* strain APA766 carrying the pKMW7 Tn5 vector library (Wetmore et al. 2015). Each vertical bar in the map represents the number of insertions within a 1000 bp region; bar height is directly proportional to the number of insertions, with approximately 1700 insertions being represented by the longest bar. Library sequencing revealed 103169 insertions in 58869 distinct locations within the JB232 genome. These insertions occur within the central 10-90% of each represented gene. The RB-TnSeq library contains mutants in approximately 88% of the protein-coding genes, each of which has an average of 25.6 strains. The insertion map was visualized using Anvi'o.

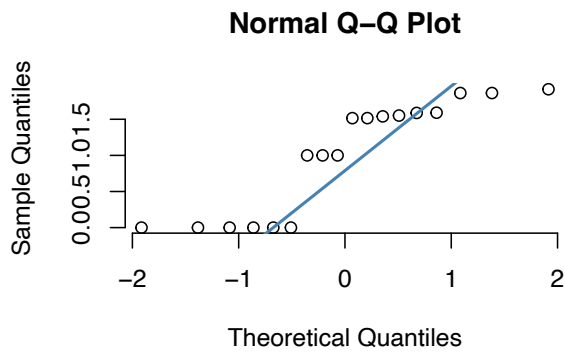


**Supplementary Figure 3.2. Comparison of significant gene fitness values for the individual replicates in each experimental condition.** (A) Principal Component Analysis was conducted on the significant gene fitness values using the `prcomp()` function in Rstudio. (B) We identified genes of significant fitness unique to and/or shared by the three replicates from four growth conditions using the UpSetR package in Rstudio (Lex et al. 2014, Conway et al. 2017).

**A**



**B**



**Supplementary Figure 3.3.** Determining the normality of the data sets visualized in Figure 4. (A) Under all tested conditions, the number of *Hafnia* colony forming units follows a normal distribution based on Shapiro-Wilk (S-W) and Pearson Chi-Squared Normality tests ( $p > 0.05$ ). (B) The number of plaque-forming units of TS33 does not follow a normal distribution based on the shape of the quantile-quantile plot ( $p < 0.05$ ).

**Supplementary Table 3.1.** *Hafnia* sp. JB232 mutants isolated from barcoded transposon mutant library. All mutants have mutations in genes related to LPS biosynthesis.

<b>Strain Name</b>	<b>Disrupted Gene</b>	<b>Susceptibility to TS33</b>
1	<i>wzy</i>	NONE
2	<i>wzy</i>	NONE
3	<i>wzy</i>	NONE
4	<i>wzy</i>	NONE
5	<i>wzy</i>	NONE
6	<i>wzy</i>	NONE
7	<i>wzy</i>	NONE
8	<i>wzy</i>	NONE
9	<i>manC</i>	DECREASED
10	<i>rfaL</i>	DECREASED
11	<i>manC</i>	DECREASED
12	<i>wzy</i>	NONE
13	Glycosyltransferase involved in cell wall biosynthesis	DECREASED
14	<i>wzy</i>	NONE
15	<i>wzy</i>	NONE
16	<i>wzy</i>	NONE
17	<i>wzy</i>	NONE
18	<i>noeK</i>	DECREASED
19	<i>manC</i>	DECREASED
20	<i>manC</i>	DECREASED
21	<i>manC</i>	DECREASED
22	<i>wzy</i>	NONE
23	Glycosyltransferase involved in cell wall biosynthesis	DECREASED
24	Glycosyltransferase involved in cell wall biosynthesis	DECREASED
25	<i>wzy</i>	NONE
26	<i>wzy</i>	NONE
27	<i>manC</i>	DECREASED
28	<i>wzy</i>	NONE
29	<i>wzy</i>	NONE

**Supplementary Table 3.1.** *Hafnia* sp. JB232 mutants isolated from barcoded transposon mutant library. All mutants have mutations in genes related to LPS biosynthesis.

30	<i>wzy</i>	DECREASED
31	<i>wzy</i>	NONE
32	<i>wzy</i>	NONE
33	<i>wzy</i>	NONE
34	Glycosyltransferase involved in cell wall biosynthesis	DECREASED
35	<i>wzy</i>	NONE
36	<i>wzy</i>	NONE
37	<i>manC</i>	DECREASED
38	<i>wzy</i>	NONE
39	<i>wzy</i>	NONE
40	<i>wzy</i>	NONE
41	<i>wzy</i>	NONE
42	<i>rfaL</i>	DECREASED
43	<i>wzy</i>	NONE
44	<i>rfaH</i>	DECREASED
45	<i>rfaL</i>	DECREASED
46	<i>manC</i>	DECREASED
47	<i>manC</i>	DECREASED
48	<i>manC</i>	DECREASED
49	Glycosyltransferase involved in cell wall biosynthesis	DECREASED
50	Transposon inserted into intergenic region	NONE

“Chapter 3, in full, is currently being prepared for publication. The dissertation author was the primary research/author of this paper.”

## CHAPTER 4

### 4.1 Future Directions

#### **Molecular mechanisms of host-phage interactions within a community**

The field of community-host-phage interactions is slowly growing. Primarily, our knowledge of the specific impacts of community presence of the densities, interactions and co-evolution of bacteriophages excludes the molecular bases of these impacts. As discussed in Chapter 1, interactions between phages and various bacterial species, including *Pseudomonas* and *Klebsiella* can take a turn for the worse in the presence of the community. Host and phage suppression are common observations in these studies, many of which include an environment or community closely mimicking the natural ecosystem of the focal bacteria, with only one known exception (Alseth et al., 2019, Johnke et al., 2017, Mumford & Friman 2016, Gómez & Buckling 2011). Moreover, there are examples in the literature of both positive and negative effects of community on interactions between bacteria and phage. The available experimental results suggest that host-phage interactions experience diverse impacts from communities, but the studies supporting these data are few. Even more sparse are mechanistic evaluations of community impact on host-phage interactions. To our knowledge, the only available insight into the molecular basis of these interactions is found in the role of quorum sensing in mediating antagonistic interactions between host and phage.

The work presented here is therefore among the first that exposes the molecular underbelly of host-virus interactions within a community context. Based on the results presented in Chapter 3, it appears that the LPS, especially the O-antigen, lies at the heart of community-virus-host interactions. In our experiments, we demonstrate that the *Hafnia* LPS is a potential attachment site for phage TS33, as is the case for other phages (Letarov and Kulikov 2017).

Moreover, the phage most likely adsorbs to the O-antigen (Figure 4A, Figure 4D, Broeker and Barbirz 2017). Simultaneously, we demonstrate that the phage-selected LPS mutants are more sensitive to fungal activity (Figure 5). Our data suggest that the community of fungi apply negative selection pressures, possibly oxidative and antibiotic on *Hafnia*, the negative effects of which are enhanced when the LPS of *Hafnia* is compromised (Pierce et al., 2020).

While previous studies showed the effects of LPS disruption on bacterial sensitivity to toxic chemicals, the toxins used in these studies do not directly originate from a microbial community member (Burmeister et al., 2020, Zhong et al., 2020). However, they are likely to be produced by other community members like fungi or other bacterial species. Detailed understanding of the molecular mechanisms underlying host-phage-community interactions warrants confirmation of the specific means by which the fungi suppress LPS-deficient *Hafnia*. Fungal genetics as well as mass spectrometry can be used to identify fungal genes and products, respectively, whose activities lead to decreased *Hafnia* growth. Furthermore, it may be worthwhile to investigate the role of other LPS components, such as Lipid A and the core polysaccharide, in mediating host-virus-community interactions.

Moreover, *Hafnia* is a representative of Gram-negative bacteria. Most known phages that infect Gram-positive bacteria primarily rely on the pilus, flagellum or a cell-surface receptor (Esteves and Scharf 2022, Rostøl and Marraffini 2019, Jacobson 1972). There is evidence that receptor mutations can increase bacterial sensitivity to antibiotics (Chan et al., 2016). Nevertheless, a holistic approach to understanding which molecular systems modulate host-phage interactions in a community context requires experiments on both groups of bacteria. It is also prudent to compare these effects to determine whether cell structures unique to both groups affect community impacts.

Finally, exploring positive interactions between communities, hosts and phages is critical. Both our data and that of others suggest that all LPS mutations do not trigger antagonistic interactions with the environment. In fact, in one study, antibiotic susceptibility is observed in LPS core oligosaccharide, but not in Lipid A mutants (McGee et al., 2023). In fact, our work shows that disruption of the third LPS component, the O-antigen, results in negative fitness effects in the presence of the community. These results suggest that the lipid core may not play a significant role in mediating bacteria-antibiotic-phage interactions. Complementation of the genes missing in these mutants may be useful in solidifying the molecular pathways involved in the interactions.

### **How does the phage infection impact the community**

Yet another poorly understood aspect of microbial ecology is the impact of phage activity on the community. As discussed in Chapter 1, phages drive host diversification, niche adaptation and abundance. Undoubtedly, these perturbations have the potential to impact the community if they affect the ecological role of the host. However, only a few studies investigate phage impacts on communities. In a simulation of spatially distributed habitats, phages were found to limit community evolution in a chemotaxis-dependent manner (Klimenko et al., 2016). Moreover, soil microbiomes reveal positive impacts of bacteriophages on nitrogen availability (Braga et al., 2020).

In our experiment, we see no significant impacts on the growth of the fungi in the presence of the *Hafnia*-TS33 interactions. However, it is possible that these impacts are being felt on the genetic level and can be quantitatively determined using fungal genetics. Throughout our community growth experiments, the abundance of the *Hafnia* library is minimally affected by fungal presence. Yet, we observe fitness effects of the fungi on the *Hafnia* mutants;

particularly, LPS mutants experience a fitness deficit. In the future, we may benefit from RNA-Seq experiments to determine changes in fungal gene expression in the presence of host-phage interactions.

## REFERENCES

1. Comeau AM, Krisch HM. 2008. The Capsid of the T4 Phage Superfamily: The Evolution, Diversity, and Structure of Some of the Most Prevalent Proteins in the Biosphere. *Molecular Biology and Evolution*. 25:1321-1332. doi:10.1093/molbev/msn080, PMID: 18391067.
2. Kauffman KM, Chang WK, Brown JM, Hussain FA, Yang J, Polz MF, Kelly L. 2022. *Nature Communications*. Resolving the structure of phage–bacteria interactions in the context of natural diversity. 13:372. doi:10.1038/s41467-021-27583-z, PMID: 35042853.
3. Jessup CM, Forde SE. 2008. Ecology and evolution in microbial systems: the generation and maintenance of diversity in phage-host interactions. *Research in Microbiology*. 5:382-389. doi:10.1016/j.resmic.2008.05.006, PMID: 18582563.
4. López-Leal G, Camelo-Valera LC, Hurtado-Ramírez JM, Verleyen J, Castillo-Ramírez S, Reyes-Muñoz A. 2022. *mSystems*. 7:e0032622. doi: 10.1128/msystems.00326-22, PMID: 35880895.
5. Norman JM, Handley SA, Baldrige MT, Droit L, Liu CY, Keller BC, Kambal A, Monaco CL, Zhao G, Fleshner P, Stappenback TS, McGovern DPB, Keshavarzian A, Mutlu EA, Sauk J, Gevers D, Xavier RJ, Wang D, Parkes M, Virgin HW. 2015. Disease-specific Alterations in the Enteric Virome in Inflammatory Bowel Disease. *Cell*. 160: 447–460. doi: 10.1016/j.cell.2015.01.002, PMID: 25619688.
6. Bondy-Denomy J, Qian J, Westra ER, Buckling A, Guttman DS, Davidson AR, Maxwell KL. 2016. Prophages mediate defense against phage infection through diverse mechanisms. *ISME Journal*. 10:2854-2866. doi: 10.1038/ismej.2016.79, PMID: 27258950.

7. Owen SV, Wenner N, Dulberger CL, Rodwell EV, Bowers-Barnard A, Quinones-Olvera N, Rigden DJ, Rubin EJ, Garner EC, Baym M, Hinton JCD. 2021. Prophages encode phage-defense systems with cognate self-immunity. *Cell Host Microbe*. 29:1620-1633.e8. doi: 10.1016/j.chom.2021.09.002, PMID: 34597593.
8. LeGault KN, Barth ZN, DePaola P IV, Seed KD. 2022. A phage parasite deploys a nicking nuclease effector to inhibit viral host replication. *Nucleic Acids Research*. 50:8401-8417. doi: 10.1093/nar/gkac002, PMID: 35066583.
9. Habets A, Antoine C, Wagemans J, Vermeersch M, Laforêt F, Diderich J, Lavigne R, Mainil J, Thiry D. 2022. Impact of Shiga-toxin encoding gene transduction from O80:H2 Shiga toxigenic *Escherichia coli* (STEC) on non-STEC strains. *Scientific Reports*. 12:21587. doi: 10.1038/s41598-022-26198-8, PMID: 36517572.
10. Fortier L. Chapter Five - The Contribution of Bacteriophages to the Biology and Virulence of Pathogenic Clostridia. 2017. *Advances in Applied Microbiology*. 101:169-200. doi:10.1016/bs.aambs.2017.05.002, PMID: 29050666.
11. Huang A, Friesen J, Brunton JL. 1987. Characterization of a bacteriophage that carries the genes for production of Shiga-like toxin 1 in *Escherichia coli*. *Journey of Bacteriology*. 169:4308-12. doi:10.1128/jb.169.9.4308-4312.1987, PMID: 3040688.
12. Yu J, Xu X, Wang Y, Zhai X, Pan Z, Jiao X, Zhang Y. 2022. Prophage-mediated genome differentiation of the *Salmonella* Derby ST71 population. *Microbial Genomics*. 8:000817. doi:10.1099/mgen.0.000817, PMID: 35451954.
13. Warwick-Dugdale J, Buchholz HH, Allen MJ, Temperton B. 2019. Host-hijacking and planktonic piracy: how phages command the microbial high seas. *Virology Journal*. 16:15. doi:10.1186/s12985-019-1120-1, PMID: 30709355.

14. Chaikeeratisak V, Nguyen K, Khanna K, Brilot AF, Erb ML, Coker JKC, Vavilina A, Newton GL, Buschauer R, Pogliano K, Villa E, Agard DA, Pogliano J. 2017. Assembly of a nucleus-like structure during viral replication in bacteria. *Science*. 355:194-197. doi: 10.1126/science.aal2130, PMID: 28082593.
15. Zdrojewska K, Dydecka A, Nejman-Faleńczyk B, Topka G, Necel A, Węgrzyn A, Węgrzyn G, Bloch S. 2019. Role of orf73 in the development of lambdoid bacteriophages during infection of the *Escherichia coli* host. *Acta biochimica Polonica*. 66:589-596. doi: 10.18388/abp.2019\_2886, PMID: 31769953.
16. Sharon I, Alperovitch A, Rohwer F, Haynes M, Glaser F, Atamna-Ismaeel N, Pinter RY, Partensky F, Koonin EV, Wolf YI, Nelson N, Béjà O. 2009. Photosystem I gene cassettes are present in marine virus genomes. *Nature*. 461:258-262. doi: 10.1038/nature08284, PMID: 19710652.
17. Alperovitch-Lavy A, Sharon I, Rohwer F, Aro E, Glaser F, Milo R, Nelson N, Béjà O. 2011. Reconstructing a puzzle: existence of cyanophages containing both photosystem-I and photosystem-II gene suites inferred from oceanic metagenomic datasets. *Environmental Microbiology*. 13:24-32. doi: 10.1111/j.1462-2920.2010.02304.x, PMID: 20649642.
18. Mann NH, Cook A, Millard A, Bailey S, Clokie M. 2003. Marine ecosystems: bacterial photosynthesis genes in a virus. *Nature*. 424:741. doi: 10.1038/424741a, PMID: 12917674.
19. Thompson LR, Zeng Q, Chisholm SW. 2016. Gene Expression Patterns during Light and Dark Infection of *Prochlorococcus* by Cyanophage. *PLoS One*. 11:e0165375. doi: 10.1371/journal.pone.0165375, PMID: 27788196.

20. Enav H, Mandel-Gutfreund Y, Béjà O. 2014. Comparative metagenomic analyses reveal viral-induced shifts of host metabolism towards nucleotide biosynthesis. *Microbiome*. 2:9. doi: 10.1186/2049-2618-2-9, PMID: 24666644.
21. Høyland-Kroghsbo NM, Paczkowski J, Mukherjee S, Broniewski J, Westra E, Bondy-Denomy J, Bassler BL. 2017. Quorum sensing controls the *Pseudomonas aeruginosa* CRISPR-Cas adaptive immune system. *PNAS*. 114:131-135. doi: 10.1073/pnas.1617415113, PMID: 27849583.
22. Shah M, Taylor VL, Bona D, Tsao Y, Stanley SY, Pimentel-Elardo SM, McCallum M, Bondy-Denomy J, Howell PL, Nodwell JR, Davidson AR, Moraes TF, Maxwell KL. 2021. A phage-encoded anti-activator inhibits quorum sensing in *Pseudomonas aeruginosa*. *Molecular Cell*. 81:571-583.e6. doi: 10.1016/j.molcel.2020.12.011, PMID: 33412111.
23. van Kessel JC, Mukherjee S. 2021. Another battle won in the phage-host arms race: *Pseudomonas* phage blocks quorum sensing regulator LasR. *Molecular Cell*. 81:420-422. doi: 10.1016/j.molcel.2021.01.007, PMID: 33545057.
24. Fernández L, González S, Campelo AB, Martínez B, Rodríguez A, Pilar García P. 2017. Low-level predation by lytic phage phiIPLA-RODI promotes biofilm formation and triggers the stringent response in *Staphylococcus aureus*. *Scientific Reports*. 7:40965. doi:10.1038/srep40965, PMID:28102347.
25. Biller SJ, Schubotz F, Roggensack SE, Thompson AW, Summons RE, Chisholm SW. 2014. Bacterial vesicles in marine ecosystems. *Science*. 343:183-186. doi: 10.1126/science.1243457, PMID: 24408433.

26. Mozaheb N, Mingeot-Leclercq. 2020. Membrane Vesicle Production as a Bacterial Defense Against Stress. *Frontiers in Microbiology*. 11:600221. doi: 10.3389/fmicb.2020.600221, PMID: 33362747.
27. Silva TP, Gamalier JP, Zarantonello V, Soares CR, Resende NS, Barros NO, Melo RCN. 2022. Enhanced ability of freshwater bacteria to secrete extracellular vesicles upon interaction with virus. *Environmental Microbiology*. 24:5882-5897. doi: 10.1111/1462-2920.16166, PMID: 35064062.
28. Williams HTP. 2013. Phage-induced diversification improves host evolvability. *BMC Evolutionary Biology*. 13:17. doi: 10.1186/1471-2148-13-17, PMID: 23339571.
29. Kortright KE, Chan BK, Evans BR, Turner PE. 2022. Arms race and fluctuating selection dynamics in *Pseudomonas aeruginosa* bacteria coevolving with phage OMKO1. *Journal of Evolutionary Biology*. 35:1475-1487. doi: 10.1111/jeb.14095, PMID:36168737.
30. Rodriguez-Valera F, Martin-Cuadrado A-B, Rodriguez-Brito B, Pasić L, Thingstad TF, Rohwer F, Mira. 2009. Explaining microbial population genomics through phage predation. *Nature Reviews Microbiology*. 7:828–836. doi: 10.1038/nrmicro2235, PMID:19834481.
31. Meyer JR, Dobias DT, Weitz JS, Barrick JE, Quick RT, Lenski RE. 2012. Repeatability and contingency in the evolution of a key innovation in phage lambda. 335:428-432. doi: 10.1126/science.1214449, PMID: 22282803.
32. Scanlan PD. 2017. Bacteria–Bacteriophage Coevolution in the Human Gut: Implications for Microbial Diversity and Functionality. *Trends in Microbiology*. 25:614-623. doi: 10.1016/j.tim.2017.02.012, PMID: 28342597.

33. Maslov S, Sneppen K. 2017. Population cycles and species diversity in dynamic Kill-the-Winner model of microbial ecosystems. *Scientific Reports*. 7:39642. doi: 10.1038/srep39642, PMID: 28051127.
34. Paterson S, Vogwill T, Buckling A, Benmayor R, Spiers AJ, Thomson NR, Quail M, Smith F, Walker D, Libberton B, Fenton A, Hall N, Brockhurst MA. 2010. Antagonistic coevolution accelerates molecular evolution. *Nature*. 464:275-8. doi: 10.1038/nature08798, PMID: 20182425.
35. Cairns J, Frickel J, Jalasvuori M, Hiltunen T, Becks L. 2017. Genomic evolution of bacterial populations under coselection by antibiotics and phage. *Molecular Ecology*. 26:1848-1859. doi: 10.1111/mec.13950, PMID: 27977892.
36. Scanlan PD, Hall AR, Blackshields G, Friman V-P, Davis Jr MR, Goldberg JB, Buckling A. 2015. Coevolution with bacteriophages drives genome-wide host evolution and constrains the acquisition of abiotic-beneficial mutations. *Molecular Biology and Evolution*. 32:1425-35. doi: 10.1093/molbev/msv032, PMID: 25681383.
37. Koskella B, Brockhurst MA. 2014. Bacteria–phage coevolution as a driver of ecological and evolutionary processes in microbial communities. *FEMS Microbiology Reviews*. 38:916-31. doi: 10.1111/1574-6976.12072, PMID: 24617569.
38. Watson BNJ, Steens JA, Staals RHJ, Westra ER, van Houte S. 2021. Coevolution between bacterial CRISPR-Cas systems and their bacteriophages. *Cell Host & Microbe*. 29:715-725. doi: 10.1016/j.chom.2021.03.018, PMID: 33984274.
39. Mojica FJM, Díez-Villaseñor C, García-Martínez J, Soria E. 2005. Intervening sequences of regularly spaced prokaryotic repeats derive from foreign genetic elements. *Journal of Molecular Evolution*. 60:174-82. doi: 10.1007/s00239-004-0046-3, PMID: 15791728.

40. Amitai G, Sorek R. 2016. CRISPR-Cas adaptation: insights into the mechanism of action. *Nature Reviews Microbiology*. 14:67-76. doi: 10.1038/nrmicro.2015.14, PMID: 26751509.
41. Garneau JE, Dupuis M-È, Villion M, Romero DA, Barrangou R, Boyaval P, Fremaux C, Horvath P, Magadán AH, Moineau S. 2010. The CRISPR/Cas bacterial immune system cleaves bacteriophage and plasmid DNA. *Nature*. 468:67-71. doi: 10.1038/nature09523. PMID: 21048762.
42. Broniewski JM, Meaden S, Paterson S, Buckling A, Westra ER. 2020. The effect of phage genetic diversity on bacterial resistance evolution. *ISME*. 14:828-836. doi: 10.1038/s41396-019-0577-7. PMID: 31896785.
43. Millman A, Melamed S, Leavitt A, Doron S, Bernheim A, Hör J, Garb J, Bechon N, Brandis A, Lopatina A, Ofir G, Hochhauser D, Stokar-Avihail A, Tal N, Sharir S, Voichek M, Erez Z, Ferrer JLM, Dar D, Kacen A, Amitai G, Sorek R. 2022. An expanded arsenal of immune systems that protect bacteria from phages. *Cell*. 30:1556-1569.e5. doi: 10.1016/j.chom.2022.09.017. PMID: 36302390.
44. Guo L, Sattler L, Shafqat S, Graumann PL, Bramkamp M. 2021. A Bacterial Dynammin-Like Protein Confers a Novel Phage Resistance Strategy on the Population Level in *Bacillus subtilis*. *mBio*. 13:e0375321. doi: 10.1128/mbio.03753-21. PMID: 35164550.
45. Rostøl JT, Marraffini L. 2019. (Ph)ighting Phages: How Bacteria Resist Their Parasites. *Cell Host Microbe*. 25:184-194. doi: 10.1016/j.chom.2019.01.009. PMID: 30763533.
46. Labrie SJ, Samson JE, Moineau S. 2010. Bacteriophage resistance mechanisms. *Nature Reviews Microbiology*. 8:317-327. doi: 10.1038/nrmicro2315. PMID: 20348932.

47. Meyer JR, Dobias DT, Weitz JS, Barrick JE, Quick RT, Lenski RE. 2012. Repeatability and contingency in the evolution of a key innovation in phage lambda. *Science*. 335:428-432. doi: 10.1126/science.1214449. PMID: 22282803.
48. Bertani B, Ruiz N. 2018. Function and Biogenesis of Lipopolysaccharides. *EcoSal Plus*. 8:10.1128/ecosalplus.ESP-0001-2018. doi: 10.1128/ecosalplus.ESP-0001-2018. PMID: 30066669.
49. Burmeister AR, Fortier A, Roush C, Lessing AJ, Bender RG, Barahman R, Grant R, Chan BK, Turner PE. 2020. Pleiotropy complicates a trade-off between phage resistance and antibiotic resistance. *PNAS*. 117:11207-11216. doi: 10.1073/pnas.1919888117. PMID: 32424102.
50. Zhong Z, Emond-Rheault J-G, Bhandare S, Lévesque R, Goodridge L. 2020. Bacteriophage-Induced Lipopolysaccharide Mutations in *Escherichia coli* Lead to Hypersensitivity to Food Grade Surfactant Sodium Dodecyl Sulfate. *Antibiotics*. 9:552. doi: 10.3390/antibiotics9090552. PMID: 32872188.
51. Kulikov EE, Golomidova AK, Prokhorov NS, Ivanov PA, Letarov AV. 2019. High-throughput LPS profiling as a tool for revealing of bacteriophage infection strategies. *Science Reports*. 9:2958. doi: 10.1038/s41598-019-39590-8. PMID: 30814597.
52. Hancock RE, Reeves P. 1976. Lipopolysaccharide-deficient, bacteriophage-resistant mutants of *Escherichia coli* K-12. *Journal of Bacteriology*. 127:98-108. doi: 10.1128/jb.127.1.98-108.1976. PMID: 776951.
53. Falkowski PG, Fenchel T, Delong EF. 2008. The microbial engines that drive Earth's biogeochemical cycles. *Science*. 320:1034-1039. doi: 10.1126/science.1153213. PMID: 18497287.

54. Fung TC, Olson CA, Hsiao EY. 2017. Interactions between the microbiota, immune and nervous systems in health and disease. *Nature Neuroscience*. 20:145-155. doi: 10.1038/nn.4476. PMID: 28092661.
55. Urakova N, Joseph RE, Huntsinger A, Macias VM, Jones MJ, Sigle LT, Li M, Akbari OS, Xi Z, Lympelopoulos K, Sayre RT, McGraw EA, Rasgon JL. 2022. Alpha-mannosidase-2 modulates arbovirus infection in a pathogen- and *Wolbachia*-specific manner in *Aedes aegypti* mosquitoes. *bioRxiv*. doi: 10.1101/2022.03.18.484928.
56. Walker T, Johnson PH, Moreira LA, Iturbe-Ormaetxe I, Frentiu FD, McMeniman CJ, Leong YS, Dong Y, Axford J, Kriesner P, Lloyd AL, Ritchie SA, O'Neill SL, Hoffmann AA. 2011. The wMel *Wolbachia* strain blocks dengue and invades caged *Aedes aegypti* populations. *Nature*. 476:450-3. doi: 10.1038/nature10355. PMID: 21866159.
57. Sekerci Y, Petrovskii S. 2015. Mathematical Modelling of Plankton-Oxygen Dynamics Under the Climate Change. *Bulletin of Mathematical Biology*. 77:2325-2353. doi: 10.1007/s11538-015-0126-0. PMID: 26607949.
58. Gómez P, Buckling A. 2011. Bacteria-phage antagonistic coevolution in soil. *Science*. 332:106-109. doi: 10.1126/science.1198767. PMID: 21454789.
59. Mumford R, Friman V. 2016. Bacterial competition and quorum-sensing signalling shape the eco-evolutionary outcomes of model in vitro phage therapy. *Evolutionary Applications*. 10:161-169. doi: 10.1111/eva.12435. PMID: 28127392.
60. Alseth E, Pursey E, Luján A, McLeod I, Rollie C, Westra E. 2019. Bacterial biodiversity drives the evolution of CRISPR-based phage resistance. *Nature*. 574:549-552. doi: 10.1038/s41586-019-1662-9. PMID: 31645729.

61. Johnke J, Baron M, de Leeuw M, Kushmaro A, Jurkevitch E, Harms H and Chatzinotas A. 2017. A Generalist Protist Predator Enables Coexistence in Multitrophic Predator-Prey Systems Containing a Phage and the Bacterial Predator *Bdellovibrio*. *Frontiers in Ecology and Evolution*. 5:124. doi: 10.3389/fevo.2017.00124.
62. Blazanin M, Turner P. 2021. Community context matters for bacteria-phage ecology and evolution. *ISME*. 15:3119-3128. doi: 10.1038/s41396-021-01012-x. PMID: 34127803.
63. Middelboe M, Hagström A, Blackburn N, Sinn B, Fischer U, Borch NH, Pinhassi J, Simu K, Lorenz MG. 2001. Effects of Bacteriophages on the Population Dynamics of Four Strains of Pelagic Marine Bacteria. *Microbial Ecology*. 42:395-406. doi: 10.1007/s00248-001-0012-1. PMID: 12024264.
64. De Sorti L, Lourenço M, Laurent D. 2019. "I will survive": A tale of bacteriophage-bacteria coevolution in the gut. *Gut Microbes*. 10:92-99. doi: 10.1080/19490976.2018.1474322. PMID: 29913091.
65. De Sorti L, Khanna V, Laurent D. 2017. The Gut Microbiota Facilitates Drifts in the Genetic Diversity and Infectivity of Bacterial Viruses. *Cell Host Microbe*. 22:801-808.e3. doi: 10.1016/j.chom.2017.10.010. PMID: 29174401.
66. Middelboe M, Holmfeldt K, Riemann L, Nybroe O, Haaber J. 2009. Bacteriophages drive strain diversification in a marine Flavobacterium: implications for phage resistance and physiological properties. *Environmental Microbiology*. 11:1971-82. doi: 10.1111/j.1462-2920.2009.01920.x. PMID: 19508553.
67. Avrani S, Wurtzel O, Sharon I, Sorek R, Lindell D. 2011. Genomic island variability facilitates *Prochlorococcus*-virus coexistence. *Nature*. 474:604-608. doi: 10.1038/nature10172. PMID: 21720364.

68. Marston MF, Pierciey FJ, Shepard A, Gearin G, Qi J, Yandava C, Schuster SC, Henn MR, Martiny JBH. 2012. Rapid diversification of coevolving marine *Synechococcus* and a virus. *PNAS*. 109:4544-4549. doi: 10.1073/pnas.1120310109. PMID: 22388749.
69. Brockhurst MA, Buckling A, Rainey PB. 2005. The effect of a bacteriophage on diversification of the opportunistic bacterial pathogen, *Pseudomonas aeruginosa*. *Proceedings of the Royal Society B*. 272:1385-1391. doi: 10.1098/rspb.2005.3086. PMID: 16006335.
70. Pagnout C, Sohm B, Razafitianamaharavo A, Caillet C, Offroy M, Leduc M, Gendre H, Jomini S, Beaussart A, Bauda P, Duval JFL. 2019. Pleiotropic effects of *rfa*-gene mutations on *Escherichia coli* envelope properties. *Nature*. 9:9696. doi: 10.1038/s41598-019-46100-3. PMID: 31273247.
71. Chan BK, Siström M, Wertz JE, Kortright KE, Narayan D, Turner PE. 2016. Phage selection restores antibiotic sensitivity in MDR *Pseudomonas aeruginosa*. *Science Reports*. 6:26717. doi: 10.1038/srep26717. PMID: 27225966.
72. McGee LW, Barhoush Y, Shima R, Hennessy M. 2023. Phage-resistant mutations impact bacteria susceptibility to future phage infections and antibiotic response. *Ecology and Evolution*. 13:e9712. doi: 10.1002/ece3.9712. PMID: 36620417.
73. Wolfe BE, Button JE, Santarelli M, Dutton R. 2014. Cheese rind communities provide tractable systems for in situ and in vitro studies of microbial diversity. *Cell*. 158:422-433. doi: 10.1016/j.cell.2014.05.041. PMID: 25036636.
74. Saak CC, Pierce EC, Dinh CB, Portik D, Hall R, Ashby M, Dutton RJ. 2023. Longitudinal, Multi-Platform Metagenomics Yields a High-Quality Genomic Catalog and

- Guides an In Vitro Model for Cheese Communities. *mSystems*. 8:e0070122. doi: 10.1128/msystems.00701-22. PMID: 36622155.
75. Morin MA, Pierce EC, Dutton RJ. 2018. Changes in the genetic requirements for microbial interactions with increasing community complexity. *eLife*. 7:e37072. doi: 10.7554/eLife.37072. PMID: 30211673.
76. Morin MA, Morrison AJ, Harms MJ, Dutton RJ. 2022. Higher-order interactions shape microbial interactions as microbial community complexity increases. *Science Reports*. 12:22640. doi: 10.1038/s41598-022-25303-1. PMID: 36587027.
77. Bonham KS, Wolfe BE, Dutton RJ. 2017. Extensive horizontal gene transfer in cheese-associated bacteria. *eLife*. 6:e22144. doi: 10.7554/eLife.22144. PMID: 28644126.
78. Pierce EC, Morin M, Little JC, Liu RB, Tannous J, Keller NP, Pogliano K, Wolfe BE, Sanchez LM, Dutton RJ. 2021. Bacterial-fungal interactions revealed by genome-wide analysis of bacterial mutant fitness. *Nature Microbiology*. 6:87-102. doi: 10.1038/s41564-020-00800-z. PMID: 33139882.
79. Wiedenbeck J, Cohan FM. 2011. Origins of bacterial diversity through horizontal genetic transfer and adaptation to new ecological niches. *FEMS Microbiology Reviews*. 35:957-976. doi: 10.1111/j.1574-6976.2011.00292.x. PMID: 21711367.
80. Koonin EV. 2012. The wonder world of microbial viruses. *Expert Review of Anti-infective Therapy*. 8:1097-1099. doi: 10.1586/eri.10.96, PMID: 20954874.
81. Manrique P, Dills M, Young MJ. 2017. The Human Gut Phage Community and Its Implications for Health and Disease. *Viruses*. 9:141. doi: 10.3390/v9060141, PMID: 28594392.

82. Pratama AA, van Elsas JD. 2018. The 'Neglected' Soil Virome - Potential Role and Impact. *Trends in Microbiology*. 26: 649-662. doi: 10.1016/j.tim.2017.12.004, PMID: 29306554.
83. Febvre HP, Rao S, Gindin M, Goodwin NDM, Finer E, Vivanco JS, Lu S, Manter DK, Wallace TC, Weir TL. 2019. PHAGE Study: Effects of Supplemental Bacteriophage Intake on Inflammation and Gut Microbiota in Healthy Adults. *Nutrients*. 11:666. doi: 10.3390/nu11030666, PMID: 30897686.
84. Homma K, Fukuchi S, Nakamura Y, Gojobori T, Nishikawa K. 2007. Gene cluster analysis method identifies horizontally transferred genes with high reliability and indicates that they provide the main mechanism of operon gain in 8 species of gamma-Proteobacteria. *Molecular Biology and Evolution*. 24:805-813. doi: 10.1093/molbev/msl206, PMID: 17185745.
85. Li F, Tian F, Nazir A, Sui S, Li M, Cheng D, Nong S, Ali A, KaKar M-U, Li L, Feng Q, Tong Y. 2022. Isolation and genomic characterization of a novel Autographiviridae bacteriophage IME184 with lytic activity against *Klebsiella pneumoniae*. *Virus Research*. 319:198873. doi: 10.1016/j.virusres.2022.198873. PMID: 35868353.
86. Bebeacua C, Lai L, Skovgaard Vegge C, Brøndsted L, van Heel M, Velesler D, Cambillau C. 2013. Visualizing a complete Siphoviridae member by single-particle electron microscopy: the structure of lactococcal phage TP901-1. *Journal of Virology*. 87:1061-1068. doi: 10.1128/JVI.02836-12. PMID: 23135714.
87. Chevallereau A, Pons BJ, van Houte S, Westra ER. 2022. Interactions between bacterial and phage communities in natural environments. *Nature*. 20:49-62. doi: 10.1038/s41579-021-00602-y. PMID: 34373631.

88. Gillespie JJ, Wattam AR, Cammer SA, Gabbard JL, Shukla MP, Dalay O, Driscoll T, Hix D, Mane SP, Mao C, Nordberg EK, Scott M, Schulman JR, Snyder RR, Sullivan DE, Wang C, Warren A, Williams KP, Xue T, Yoo HS, Zhang C, Zhang Y, Will R, Kenyon RW, Sobral BW. 2011. PATRIC: the comprehensive bacterial bioinformatics resource with a focus on human pathogenic species. *Infection and Immunity*. 79:4286-4298. doi: 10.1128/IAI.00207-11. PMID: 21896772.
89. Bankevich A, Nurk S, Antipov D, Gurevich DD, Dvorkin M, Kulikov AS, Lesin VM, Nikolenko SI, Son Pham, Prjibelski AD, Pyshkin AV, Sirotkin AV, Vyahhi N, Tesler G, Alekseyev MA, Pevzner PA. 2012. SPAdes: a new genome assembly algorithm and its applications to single-cell sequencing. *Journey of Computational Biology*. 19:455-477. doi: 10.1089/cmb.2012.0021. PMID: 22506599.
90. Darling ACE, Mau B, Blattner FR, Perna NT. 2004. Mauve: multiple alignment of conserved genomic sequence with rearrangements. *Genome Research*. 14:1394-403. doi: 10.1101/gr.2289704. PMID: 15231754.
91. Goris J, Konstantinidis KT, Klappenbach JA, Coenye T, Vandamme P, Tiedje JM. 2007. DNA-DNA hybridization values and their relationship to whole-genome sequence similarities. *International Journal of Systematic and Evolutionary Microbiology*. 57:81-91. doi: 10.1099/ijs.0.64483-0. PMID: 17220447.
92. Rodriguez-R LM, Konstantinidis KT. 2016. The enveomics collection: a toolbox for specialized analyses of microbial genomes and metagenomes. *PeerJ Preprints*. 4:e1900v1 <https://doi.org/10.7287/peerj.preprints.1900v1>.

93. Kumar S, Stecher G, Li M, Knyaz C, Tamura K. 2018. MEGA X: Molecular Evolutionary Genetics Analysis across Computing Platforms. *Molecular Biology and Evolution*. 35:1547-1549. doi: 10.1093/molbev/msy096. PMID: 29722887.
94. Nishimura Y, Yoshida T, Kuronishi M, Uehara H, Ogata H, Goto S. 2017. ViPTree: the viral proteomic tree server. *Bioinformatics*. 33:2379-2380. doi: 10.1093/bioinformatics/btx157. PMID: 28379287.
95. Meier-Kolthoff JP, Göker M. 2019. TYGS is an automated high-throughput platform for state-of-the-art genome-based taxonomy. *Nature Communications*. 10:2182. doi: 10.1038/s41467-019-10210-3. PMID: 31097708.